



Investigation of Passive Control Devices for Potential Application to a Launch Vehicle Structure to Reduce the Interior Noise Levels During Launch

Final Report for Stage 4 Task 4.5

Printed 25 May 2006

Prepared For: AFOSR
Contract Number: FA5209-05-P-0109
Purchase Request: F7AFOS42990200

Prepared by: Dr. Carl Q. Howard
Professor Colin H. Hansen
Address: School of Mechanical Engineering
The University of Adelaide
SA 5005
Australia

Report Documentation Page			Form Approved OMB No. 0704-0188		
Public reporting burden for the collection of information is estimated to average 1 hour per response, including the time for reviewing instructions, searching existing data sources, gathering and maintaining the data needed, and completing and reviewing the collection of information. Send comments regarding this burden estimate or any other aspect of this collection of information, including suggestions for reducing this burden, to Washington Headquarters Services, Directorate for Information Operations and Reports, 1215 Jefferson Davis Highway, Suite 1204, Arlington VA 22202-4302. Respondents should be aware that notwithstanding any other provision of law, no person shall be subject to a penalty for failing to comply with a collection of information if it does not display a currently valid OMB control number.					
1. REPORT DATE 29 SEP 2006		2. REPORT TYPE FInal		3. DATES COVERED 01-11-2000 to 01-05-2006	
4. TITLE AND SUBTITLE Investigation of Passive Control Devices for Potential Application to a Launch Vehicle Structure to Reduce the Interior Noise Levels During Launch			5a. CONTRACT NUMBER FA520905P0109		
			5b. GRANT NUMBER		
			5c. PROGRAM ELEMENT NUMBER		
6. AUTHOR(S) Colin Hansen			5d. PROJECT NUMBER		
			5e. TASK NUMBER		
			5f. WORK UNIT NUMBER		
7. PERFORMING ORGANIZATION NAME(S) AND ADDRESS(ES) University of Adelaide,Dept. of Mechanical Engineering,North Terrace, Adelaide, SA 5005,Australia,AU,5005			8. PERFORMING ORGANIZATION REPORT NUMBER N/A		
9. SPONSORING/MONITORING AGENCY NAME(S) AND ADDRESS(ES) AOARD, UNIT 45002, APO, AP, 96337-5002			10. SPONSOR/MONITOR'S ACRONYM(S) AOARD		
			11. SPONSOR/MONITOR'S REPORT NUMBER(S) AOARD-054022,034015,0240		
12. DISTRIBUTION/AVAILABILITY STATEMENT Approved for public release; distribution unlimited					
13. SUPPLEMENTARY NOTES					
14. ABSTRACT This series of reports document a multi-year research project into the reduction of acoustic vibrations in space launch vehicles using passive mass damping devices.					
15. SUBJECT TERMS					
16. SECURITY CLASSIFICATION OF:			17. LIMITATION OF ABSTRACT Same as Report (SAR)	18. NUMBER OF PAGES 86	19a. NAME OF RESPONSIBLE PERSON
a. REPORT unclassified	b. ABSTRACT unclassified	c. THIS PAGE unclassified			

Contents

Contents	2
Executive Summary	3
1 Introduction	6
2 Task 4.5: Summarise Earlier Stage Work	10
2.1 Summary of the Entire Project	10
2.2 Stage 1	16
2.3 Stage 2	19
2.4 Stage 3	23
2.4.1 Stage 3, Task 1	23
2.4.2 Stage 3, Task 2	27
2.5 Stage 4	30
2.5.1 Stage 4, Task 1	30
2.5.2 Stage 4, Task 2	36
2.5.3 Stage 4, Task 3	39
2.5.4 Stage 4, Task 4	47
3 Conclusions	55
3.1 Major Outcomes	55
3.2 Recommendations for Future Work	56
A Experimental Testing	58
A.1 Introduction	58
A.2 Transmission Loss of Panels	58
A.3 Experimental Testing	60
A.3.1 Introduction	60
A.3.2 Experimental Setup	60
A.3.3 Results	67
A.4 Conclusions	75
B Properties of the Acoustic Chambers	76
Publications Arising from This Project	79
References	81

Executive Summary

The work described here is directed at optimising a combination of passive vibration devices and passive acoustic devices to minimise the transmission of low frequency rocket motor noise launch vehicle fairing structures. This report contains a summary of the work undertaken in Stages 1 - 4 [1–8] of the project. Each of the four stages of the project has been reported in greater detail separately, so only a summary of the most important techniques and results is presented here.

In the stage 1 study, the optimal configuration of a Passive Vibro-Acoustic Device (PVAD) mounted to the interior of a small cylinder was investigated. The PVAD consisted of an acoustic absorber and a vibration absorber (Tuned Mass Damper, TMD) combined together into the one device, and it was mounted to a flexible aluminum panel used as the cylinder end cap. A mathematical framework was developed that used the modal analysis results from a finite element model together with a modal coupling method, to calculate the interior acoustic pressure and the vibration levels on the enclosing structure. The study found that the optimal PVAD design used the TMD essentially as a mass, as the uncoupled resonance frequency of the TMD was just below the upper bound of the frequency band of interest. The study also found that the optimal loudspeaker diaphragm configuration was highly lossy, so that it reduced the modal amplitude of a single acoustic mode.

The objectives of Stage 2 of the project were to transfer the techniques developed in stage 1 to the optimisation of structures that more realistically represent real launch vehicles; in particular, a large composite cylinder constructed at Boeing, and a Representative Small Launch Vehicle Fairing (RSLVF). The modal coupling framework was

extended to include the effects of the PVADs. A Genetic Algorithm was used to find optimum parameters for the PVADs that would reduce a cost function, which was the interior acoustic potential energy in this case. It was found that the calculation of the cost function took an excessive length of time, and attempts were made to reduce the calculation time by reducing the number of modes in the analysis. Vibration and acoustic modes that did not significantly contribute to the acoustic potential energy were removed from the analysis, which decreased the calculation time. However, this action resulted in a reduction in the number of possible optimum configurations into which the structure vibrational energy could be re-arranged to achieve acoustically poor radiating modes and thus was not considered a suitable alternative.

In stage 3 of the project, tools were developed to speed up the optimisation of the location and parameters of the PVADs on the composite Boeing cylinder. This involved creating a distributed computing network using 200 desktop computers and developing a compatible parallel genetic algorithm. The time taken to conduct the optimisations was reduced by a factor of approximately 25 compared to using a single computer. It was also found that an integer representation of the chromosomes in the genetic algorithm resulted in faster convergence to the optimum compared to that achieved when a binary string representation was used.

The first two tasks of Stage 4 involved the application of the tools developed in the previous stages to the Representative Small Launch Vehicle Fairing (RSLVF). An improved mathematical framework was also developed for calculating the vibro-acoustic response of the system, which reduced the calculation time by approximately 50%. This faster technique was used to identify trends on an example problem of a rectangular cavity with a simply supported rectangular plate, which had tuned vibration dampers attached to the plate to reduce the sound transmission into the cavity. The results showed that for a fixed mass added to the plate, the greatest noise reduction was achieved by attaching a large number of light-weight tuned vibration dampers to the plate, rather than a small number of heavy-weight tuned vibration dampers. This

latter approach also had the advantage that the noise reduction that was achieved was relatively insensitive to the location of the dampers on the plate. This method was also applied to the RSLVF and similar trends were identified.

The second task in stage 4 of the project involved developing mathematical tools to analyse multiple degree of freedom tuned vibration dampers that are capable of transmitting both translational forces and rotational moments to the structure. Optimisations were conducted to determine the noise reduction that could be achieved with these multiple degree of freedom absorbers. The results showed that for the same added mass to the fairing, the same amount of noise reduction was obtained when 20 PVADs with multiple degrees of freedom, and 500 PVADs with a single degree of freedom were used.

The third and fourth tasks in stage 4 involved the analysis of the effect of practical phenomena such as separation seams on the RSLVF, which have the effect of increasing the stiffness of the fairing structure, and exhaust vents, which have the effect of changing the acoustic modes of the fairing cavity. These analyses show that there is little change between the results obtained for the unmodified RSLVF and those corresponding to the models that incorporate the practical deviations from the basic simple structure. The effect of rigid and flexible payloads inside the fairing was also examined and it was found that the sound levels inside the fairing increased with the presence of a payload. Finally, the effect of several external acoustic loading conditions on the sound levels inside the fairing was examined. Analyses were conducted with acoustic harmonic plane waves striking the fairing at various angles of incidence, which were characterised by a predictable phase, and also acoustic waves with random phase were considered.

The purpose of this report is to collate all the knowledge that has been gained during all four stages, into a single concise document.

Chapter 1

Introduction

During the launch of a rocket vehicle containing a satellite, high sound pressure levels are generated by the rocket engines, which vibrate and possibly damage components on the satellite. Excessive noise levels inside the payload bays of launch vehicles are blamed for as many as 60% of first day satellite failures [9]. It is claimed that 40% of the mass of a satellite is present just to enable the satellite to survive the harsh vibro-acoustic launch environment [10]. These harsh acoustic conditions that impinge on the fairing only last about one minute after launch, after which time the launch vehicle is usually at an altitude where the density of the air is so low that acoustic waves no longer cause problems. Hence there is a severe weight penalty required to overcome an environment that exists for a short period compared to the life of the payload. It costs approximately \$US10,000 per pound to launch objects into space [11], and hence there are obvious financial benefits that can be realised by making satellites lighter. The main aim of this project was to investigate the effect of the application of light-weight acoustic and vibration control devices to the fairing walls in reducing the transmission of sound into the payload bay that contains a satellite. The project was divided into four primary stages with a number of sub-tasks in each stage. The current report is concerned with the final task of stage 4, which includes a summary of all the previous work undertaken in stages 1 to 3 and the first parts of stage 4.

Previous work undertaken prior the the beginning of the current project involved

an investigation of the application of active feedback control of launch vehicle structural vibration using radiation mode vibration levels as the cost function to minimise interior noise levels, and this work led to the publication of three scholarly papers. The small benefit of active control, compared to the passive effect of the un-excited actuators attached to the structure has been the impetus behind the more recent work conducted as part of the current project; which is directed at optimising the passive effect of vibration reducing devices.

In previous stages of this project, mathematical tools were developed to determine optimum parameters for the locations, stiffness, mass and damping of Helmholtz Resonators (HRs) and Tuned Mass Dampers (TMDs) attached to the circumference of a launch vehicle fairing. The combination of these two devices into a single device to control the structural vibration and acoustic response of the fairing simultaneously is called a Passive Vibro-Acoustic Device (PVAD). Finite element models were used in Stages 2 and 3A to represent a composite cylinder, which was made by Boeing and intended to represent a simplified launch vehicle fairing model. The same mathematical tools are used here to analyse a more representative fairing model referred to as the Representative Scale Launch Vehicle Fairing (RSLVF). A Nastran finite element model, which was supplied by Boeing SVS, was re-interpreted into the ANSYS finite element software package and modal analyses were conducted to extract the in-vacuo mode shapes and resonance frequencies for the structure and acoustic cavity of the RSLVF. Comparisons of the mode shapes predicted using Nastran and ANSYS were presented in the report for Stage 2 of the current project. These mode shapes and resonance frequencies were used by the Matlab modal coupling software to calculate the response of the coupled structural cavity system to a specified acoustic input. Stage 3 of the current project involved developing a distributed computing network using 200 desktop computers and developing a compatible parallel genetic algorithm for use with the distributed computing network. These two tools were used to conduct optimisations of PVADs attached to a cylinder made of composite material. In stage 4, tasks 1 and 2,

these two tools were used to conduct optimisations of PVADs attached to the RSLVF. In addition, analyses were conducted of the PVADs that had tuned-mass-dampers which were capable of imparting both translational and rotational forces to the fairing structure. It was found that these devices were very effective at reducing the sound transmitted into the fairing compared to the TMDs that only had translational degrees of freedom; however, the practical realisation of these devices would be difficult.

One of the purposes of Stage 4 Task 3 was to examine the effect of structural anomalies and acoustic fill on the acoustic levels inside the Representative Scale Launch Vehicle Fairing (RSLVF). These analyses showed that there is little change between the results obtained for the unmodified RSLVF and those corresponding to the models that incorporate the practical deviations from the basic simple structure. The effect of rigid and flexible payloads inside the fairing was also examined and it was found that the sound levels inside the fairing increased with the presence of a payload.

An optimisation technique, using a genetic algorithm, was used here to determine parameters that result in the minimisation of the global sound field inside the fairing cavity of the RSLVF. This technique is fully described in the Stage 3A [4] and Stage 3B [5] reports. The genetic algorithm was adapted for use on a distributed computing network, where unused desktop computers in a computing pool were used by the genetic algorithm to evaluate the sound field in the cavity. This distributed computing network of about 230 desktop computers had a measured computational speed of about 160 GigaFLOPS, and enabled the optimisations to be completed in a reasonable time frame.

The purpose of the remaining current task (Stage 4 Task 5) is to: *“prepare a final report documenting Stage 4 results and providing a summary of relevant earlier stage work”*.

Chapter 2 describes a brief summary of the techniques that were developed and results of analyses from the four stages of this project. Appendix A describes experimental testing of the transmission loss of a rectangular panel with tuned-vibration-dampers (TMDs) attached to the panel. Although the contract did not require experimental test-

ing, it is the opinion of the author that experimental testing would indicate validity of the theoretical models that were developed in this multi-stage project.

Chapter 2

Task 4.5: Summarise Earlier Stage Work

This task was labelled 'Stage 4 Task 5' in the proposal in which the work statement was as follows.

The contractor shall prepare a final report documenting Stage 4 results and providing a summary of relevant earlier stage work.

2.1 Summary of the Entire Project

The first report for this project was delivered to AOARD in November 2000 [1] and the project has continued to 2006. During the various stages of this project, analyses have been conducted on three types of vibro-acoustic systems: a small cylinder, the Boeing composite cylinder, and the Representative Scale Launch Vehicle Fairing (RSLVF), and involved the development of mathematic models that required the use of Finite Element Methods, Boundary Element Methods, and modal coupling theory. The tasks within each stage of the work focused on different aspects of the same noise control problem. Figure 2.1 shows a summary of the tasks in each of the 4 stages of this project.

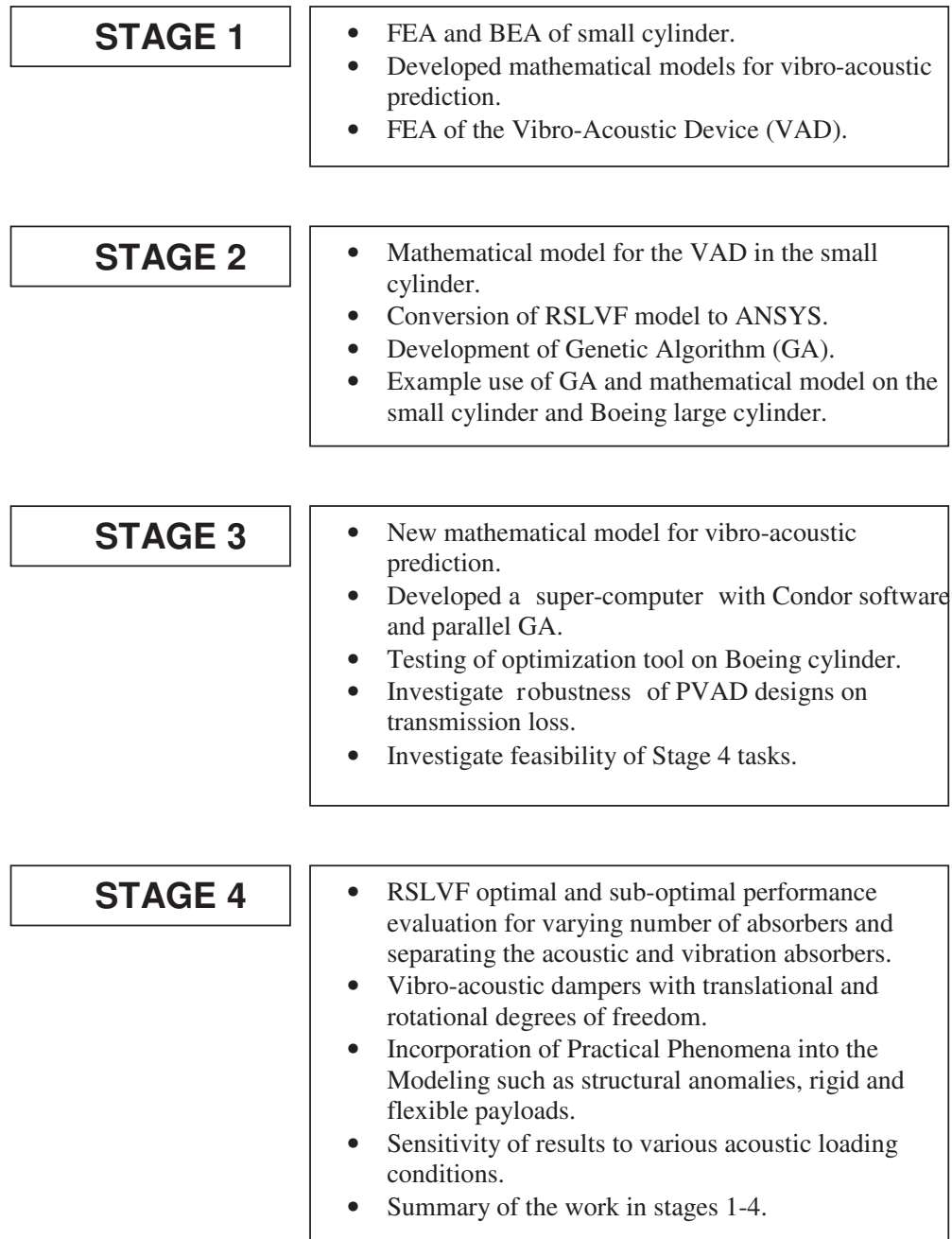


FIG. 2.1: Overview of tasks in each stage of the work.

Figure 2.2 shows an overview of the analysis tools that were developed as part of this project.

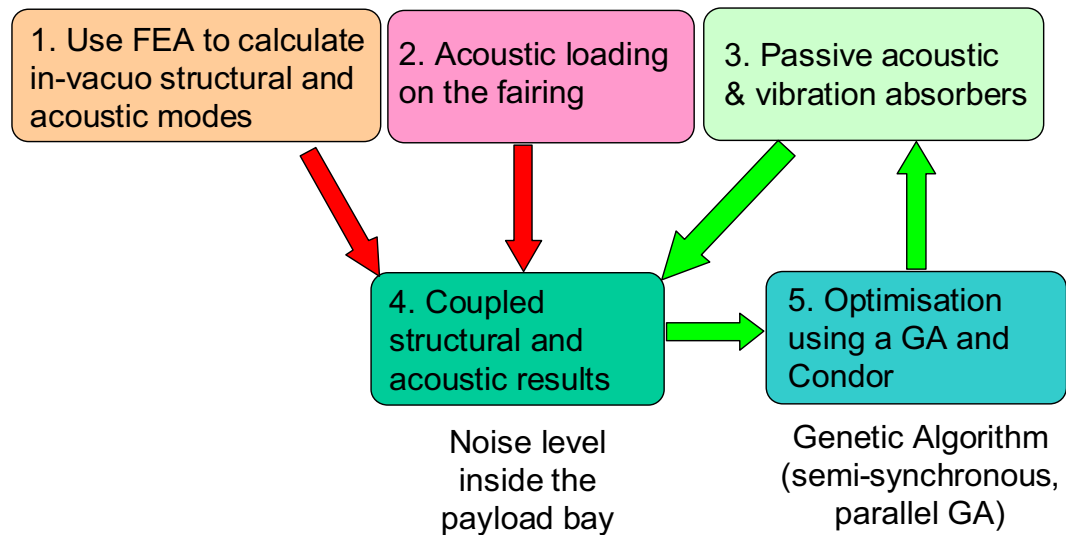


FIG. 2.2: Overview of the analysis methods.

Step 1: Use FEA to calculate in-vacuo structural and acoustic modes The early stages of the project were focused on developing finite element methods to calculate the in-vacuo modal responses of a general structure and acoustic cavity. It is well known by acousticians that theoretical analysis is only possible for ‘simple’ geometries such as rectangular boxes, or cylinders; for anything more complex in shape, numerical techniques are generally used. Similarly, for the vibration analysis of structures, apart from a simply-supported rectangular plate, most structures become difficult to model theoretically and acousticians resort to using numerical techniques such as FEA. A method was developed to extract the modal responses for the structure and the acoustic cavity and export the data in a format that would be suitable for combining using Matlab.

Step 2: Acoustic loading on the fairing Ideally it is preferable to have a representative acoustic model for the acoustic loads that act on the exterior of the fairing during launch. Rocket scientists have investigated this topic and it is clear that the acoustic field is difficult to model and is best described as a stochastic model

that is partly random and has 'coherence length scales' that are a function of distance. It became clear that derivation of a realistic acoustic model for the loading on the fairing would be a separate project in itself, and instead a relatively simple acoustic loading was used that consisted of harmonic plane waves that struck the fairing at an oblique angle of incidence, and also acoustic waves characterised by random phase that struck the fairing at an oblique angle of incidence.

Step 3: Passive acoustic and vibration absorbers Early stages of this project involved investigating the effects of passive acoustic and vibration absorbers in a cylindrical thin-walled shell using finite element analysis. That is, the entire absorber was modelled using FEA and was modelled as part of the entire vibro-acoustic system to be analysed. It was hoped that a standard optimisation toolbox within the FEA package could be used to conduct the optimisations - similar to the structural optimisation that structural engineers use to optimise the strength of parts whilst minimising the weight of a part. It was clear that the solution time to solve the vibro-acoustic system examined in this project would be unacceptably long, and so the optimisation of the absorbers would be infeasible. Instead, numerical techniques were developed to incorporate the effects of the acoustic and vibration absorbers on the vibro-acoustic system, which are orders of magnitude faster than the calculation times using FEA.

Step 4: Coupled structural and acoustic results A numerical method was developed to combine the results from Steps 1 to 3 to calculate the acoustic potential energy inside the cavity, which in simple terms means the 'average sound pressure level'. The numerical method used the modal coupling theory from Fahy [12] to combine the numerical values for the mode shapes, the acoustic loading on the fairing, and a method to combine the effects of the absorbers.

Step 5: Optimisation using a genetic algorithm and Condor A genetic algorithm is a numerical optimisation method that can be used to determine a set of parame-

ters that will minimise a function. In this case, the genetic algorithm was used to determine the locations, resonance frequencies, and damping for the tuned vibration dampers and Helmholtz resonators that would minimise the noise level inside the payload bay. A genetic algorithm was used because it has two particular advantages for the problem that is investigated here: 1) it is good at finding the 'global' minimum of a cost function, whereas gradient descent type algorithms will converge to 'local' minima in the cost function, and 2) the method is amenable to being implemented on a distributed computing network, where the evaluation of the noise level inside the payload bay for each configuration of PVADs can be conducted on numerous computers at the same time. To achieve this, a distributed computing network was created using the freely distributed software called Condor [13]. Figure 2.3 shows a schematic of the Condor distributed computing network that was created using about 270 desktop computers. When a 'slave' computer is not being used by a student, it tells the 'master' computer that it is available for use. The role of the master computer is essentially to keep a roll, and to tell the 'submitter' computer which computers are available for use. The 'submitter' computer sends its computing jobs directly to the slave computers. In this case, the submitting computer sends a Matlab program to the slave computer that calculates the acoustic potential energy inside a cavity for a particular configuration of the PVADs. The submitting computer sends numerous jobs to the slave computers and waits for the results. After the slave computer returns the results, the submitting computer uses the genetic algorithm to determine a potentially better set of parameters that could improve the results and then sends out a new set of parameters to a slave computer. This process occurs asynchronously, meaning that whenever any one slave computer returns results, the submitting computer sends out another job, and does not have to wait for all the slave computers to complete their jobs.

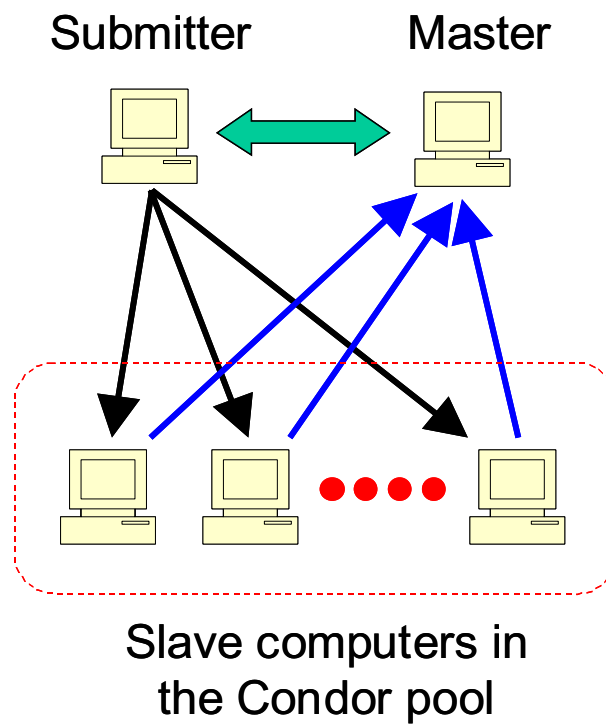


FIG. 2.3: Schematic of the distributed computing network created using the Condor software.

The following sections briefly describe the tasks in the work statement of the contracts and a brief summary of the major outcomes from each of the tasks. It should be noted that the following sections are very brief and that the reader should consult the particular relevant report for each stage to see the entire scope of work that was completed.

2.2 Stage 1

In the original proposal the work statement for this task was as follows:

1. *the analytical development of an optimally tuned acoustic/vibration absorber that could be used to reduce interior noise levels by simultaneously controlling both the interior modal response and the enclosing structural modal response.*
2. *The first stage of the project is to optimise the design of the entire device to minimise the noise transmitted into an experimental cylinder through an end cap on which the device is to be mounted.*

Major outcomes from this task were:

- This stage was the first set of work that was completed for the entire project that involved the investigation of the application of a Passive Vibro-Acoustic Device (PVAD) mounted to the interior of a small cylinder. The VAD consisted of an acoustic absorber and a vibration absorber (Tuned Mass Damper, TMD) in the one device. A picture of the steel cylinder and PVAD are shown in Figure 2.4. A finite element model of the cylinder and PVAD was created and is shown in Figure 2.5, where the PVAD is attached to the end cap of the cylinder, and the end cap of the cylinder is displaced.
- A mathematical framework was constructed that utilised the modal response of the structure and acoustic cavity that were calculated separately (in-vacuo) using the Ansys finite element software, and then coupled together in a Matlab program, to calculate the coupled response of the vibro-acoustic system.
- Analyses were conducted by selecting various configurations for the resonance frequencies, damping and mass of the tuned mass damper and the Helmholtz resonator. The results indicated that for a PVAD, the greatest noise reduction occurred when the TMD acted as a highly reactive device to reduce the structural

modal density within the frequency band of interest and the optimal diaphragm configuration was highly lossy to reduce the modal amplitude of a single acoustic mode. It should be noted that in almost all the cases considered, the equivalent mass (achieved by simply smearing the PVAD mass over the flexible panel), provided optimal passive control over a larger bandwidth. This is not surprising, since the PVAD introduces another higher order mode that boosts high frequency transmission over that achieved by the empty structure. The only benefit of the PVAD (apart from the mass loading of the primary structural mode) is the anti-resonance generated (at the uncoupled PVAD natural frequency).



FIG. 2.4: Pictures of the small steel cylinder and the PVAD made from a loudspeaker.

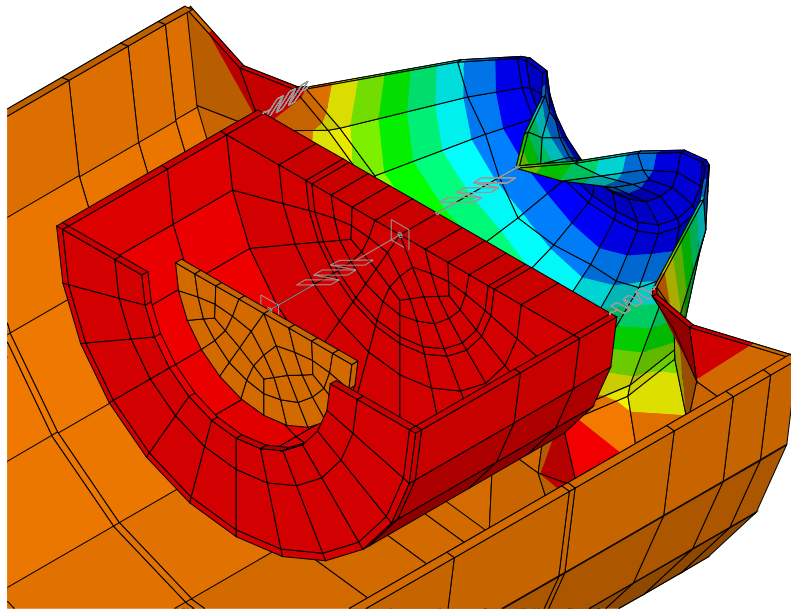


FIG. 2.5: Cross sectional view of an Ansys finite element model of the small cylinder showing a finite element model of the PVAD attached to the end cap of the cylinder, and the end cap of the cylinder is displaced.

2.3 Stage 2

In the original proposal the work statement for this task was as follows:

1. *Extend the modal coupling modeling technique developed in stage 1 to a large composite cylinder that will be tested at Boeing. This system has many more modes in the frequency range of interest (compared to the small cylinder used in stage 1) and will demonstrate the effectiveness of the modal coupling approach in analyzing a realistic structure for which fully-coupled FEA is unsuitable.*
2. *Extend the modal coupling modeling to a Representative Small Launch Vehicle Fairing (RSLVF).*
3. *Develop a model of the fairing excitation field to determine the required loading parameters for the numerical model. A steady state free-field external pressure excitation in the frequency range from 50Hz to 300Hz will be used as a first order approximation of the more complex launch environment.*
4. *Investigate the effectiveness of multi-degree-of-freedom devices in reducing sound transmission. This will involve multiple coupled elements making up a single device. The relative merits of such devices compared to simpler devices tuned to different frequencies will be evaluated.*
5. *Investigate passive absorber options for minimizing interior noise levels in a launch vehicle excited with a realistic pressure field. This task presents new challenges because in the previous tasks, a volume occupied by the PVAD was subtracted from the volume for the cavity, and then a modal analysis of the cavity was performed. In stage 1 it was assumed that the size and location of the PVAD would not change which meant that the mode shapes of the cavity would not change. If the location of the PVAD is to be optimized then the mode shape of the cavity will change slightly when the PVAD is put in the new location. An approximation will be developed for the effect of PVAD(s) location and size*

on the mode shapes of the cavity. A genetic algorithm (GA) will be used to optimize the locations of the VADs on the structure. The results achieved using reactive elements will be compared against an equivalent mass approach.

The following additional objectives were also part of this stage:

- 1. Develop models of the structural and acoustic components of the VAD that do not use the Ansys program, but allow the effect of the VAD on the frequency response to be adequately represented.*
- 2. Develop methods for reducing the computation time taken by the modal coupling method.*

The major outcomes from this task are listed below:

- Tasks 1-3 were fully completed in stage 2, as well as all of the additional tasks 1 and 2. The portion of the original task 5 relating to the implementation of Genetic Algorithms was completed, although it was found that it took a long time (1 month) for the optimisation using the genetic algorithm to achieve a near “optimal” solution. It was apparent from the work conducted in this task that significant computational power would be required to conduct these optimisations, and this was developed in Stage 3.
- Task 4 objective was not achieved due to time constraints and instead was investigated in Stage 4, Task 2 (see page 36 of this report).
- The portion of the Stage 2, task 5 relating to the effect of the VAD on the existing cavity mode shapes, was not completed because the additional task 1 required the assumption of zero additional volume. With the larger models used in this stage (the Boeing cylinder and the RSLVF), this assumption was deemed reasonable.
- The speed of calculating the acoustic potential energy in the cavity was improved by using a ‘modal thresholding’ technique, where only the modes that are strongly

coupled between the structure and the acoustic cavity were included in the analysis. However, it was later considered (in Stage 3) that the removal of the poorly coupled modes would remove potential optimal solutions, whereby the optimal configuration of the absorbers would cause a 'modal re-arrangement' of the vibration of the structure, changing the vibration energy of the structure into modes that are poor radiators of sound, and hence would result in low sound pressure levels in the cavity. Hence, in later stages, these poorly coupled modes were retained in the analyses.

- The Air Force provided a finite element model of the RSLVF in Nastran and this was converted into an equivalent model for use in the Ansys finite element analysis software.
- Boundary element analysis (BEA) software called Comet was used to calculate the pressure loading on the Boeing cylinder and the RSLVF when a point monopole source was placed along the axis of a body to simulate the noise emanating from a rocket motor. Figure 2.6 shows the results of the BEA calculation of the acoustic loading on the RSLVF at 400Hz. The pressure loads that were calculated using BEA could then be converted into equal nodal forces that act perpendicular to the surface of the structure and could be applied as the acoustic loads for the modal coupling model of the vibro-acoustic system. It was suggested that an alternative model of the acoustic loading might be more realistic. In Stage 4, Task 4, several different acoustic loading conditions were considered and the effects of varying the loading conditions on the noise levels inside the RSLVF were calculated.
- A mathematical model was developed that could be used to incorporate the effects of the acoustic and vibration absorbers in the modal-coupling of the structure and the acoustic cavity [3, p10].
- A genetic algorithm was developed in this stage that could be used to optimise the parameters for the PVADs. Unfortunately, the time taken to calculate the cost

function, the acoustic potential energy inside the cavity, was too great and optimisations were conducted using only a few (< 4 PVADs) and only 100 generations of the population. These small jobs took over 30 days and it was clear even then that the optimisation would not have been completed. As a comparison with the work that was conducted in stage 4, optimisations were conducted on the RSLVF using 500 absorbers and involved calculating 200,000 cost function evaluations at approximately 4 minutes each time on a desktop computer. In this stage 2, optimisations were conducted for the small cylinder and the Boeing cylinder, but due to a lack of computational power, were not conducted for the RSLVF. The limitations of the computational power were addressed in stage 3.

- The outcomes of this research were presented at the 9th International Congress of Sound and Vibration (see Morgans et al. [14]).

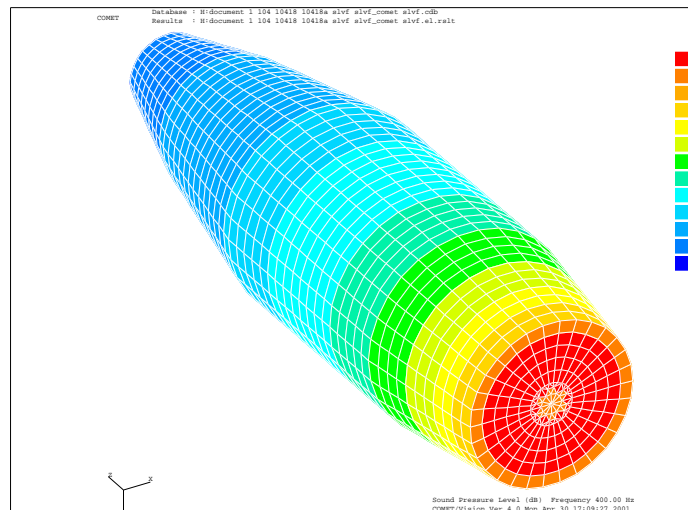


FIG. 2.6: Acoustic pressure loading on the RSLVF due to a monopole source placed along the axis of the body at 400Hz.

2.4 Stage 3

2.4.1 Stage 3, Task 1

In the original proposal the work statement for this task was as follows:

1. *Improve the Efficiency and Validity of the Design Optimisation Process.*
2. *Boeing Cylinder Optimal and Sub-optimal Performance Evaluation.*

The major outcomes from this task are listed below.

- The previous mathematical model for the vibro-acoustic system could not be easily modified to incorporate the effect of multi-degree-of-freedom acoustic and vibration absorbers. In this task, the mathematics for the coupling of the passive vibro-acoustic devices to the vibro-acoustic system was re-formulated enable the incorporation of of multi-degree of freedom absorbers, which enables the inclusion of torsional vibration for the tuned mass dampers, and multi-resonance Helmholtz resonators. This work was anticipated to commence in stage 4.
- A distributed computing network was created using the faculty's computing pool. The use of this computing network was vital for the optimisation work that was conducted in this stage. It takes about 6 minutes to calculate the cost function on a single 3.0 GHz Pentium PC. Most of the optimisations conducted in this stage of work involved calculationg 18,000 cost function evaluations. Using a single computer this would have taken about 75 days per optimisation. The use of the faculty's distributed computing network reduced the calculation time to about 3 days - 25 times faster than using a single computer.
- Several analyses were conducted to investigate the sensitivity of the interior noise reduction to parameters such as shell thickness, air temperature, acoustic damping, total mass and volume of the passive vibro-acoustic devices [4, p61]. The results show that:

- The change in air temperature from 0°C to 40°C, and hence change in speed of sound, has negligible ($< 1\text{dB}$) influence on the results [4, Fig 5.26, p63].
 - Variations in the shell thickness of $\pm 1\text{mm}$ alters the modal response of the structure, but again, this has negligible ($< 1\text{dB}$) influence on the results [4, Fig 5.29, p65].
 - Increasing the interior acoustic damping provides the greatest noise reduction compared to any method examined in this report. Figure 2.8 shows a comparison of the total acoustic potential energy inside the cylinder for the cases of without PVADs (base), and with 20 PVADs arranged into 5 rings with 4 PVADs per ring for various acoustic damping values inside the cylinder. The results show (not surprisingly) that increasing the acoustic damping within the cylinder increased the noise reduction.
- The results for the optimisation of PVADs attached to the cylinder are not particularly useful for identifying trends, as there was no fixed mass-budget and the weight of each absorber was fixed at $0.45\text{kg}=1\text{lb}$. It is not surprising that the more mass that is added to the fairing, the greater the noise reduction that could be expected. Whilst the use of a fixed mass for each absorber was consistent with experimental work that was conducted by AFOSR at Kirtland AFB in New Mexico, USA, and at Virginia Tech, Virginia, it is perhaps less useful than if the optimisation had been conducted with a fixed mass-budget, where the mass for each absorber was a fraction of the fixed mass-budget. The optimisations with a fixed mass-budget are conducted in stage 4. Nevertheless, the work that was conducted as part of this stage 3 task 1 was essential to the development of the analytical tools necessary to conduct the investigations in stage 3, task 2 and stage 4 tasks 1-4.
- The genetic algorithm that was used for the optimisation in stage 2 used an integer representation for the chromosomes. In stage 3, task 1, a binary string representation was used, which also appeared to give satisfactory results. The genetic

algorithms developed in this stage were modified for use with the distributed computing network.

- The outcomes of this research were published in the Noise Control Engineering Journal (see Howard et al. [15]).

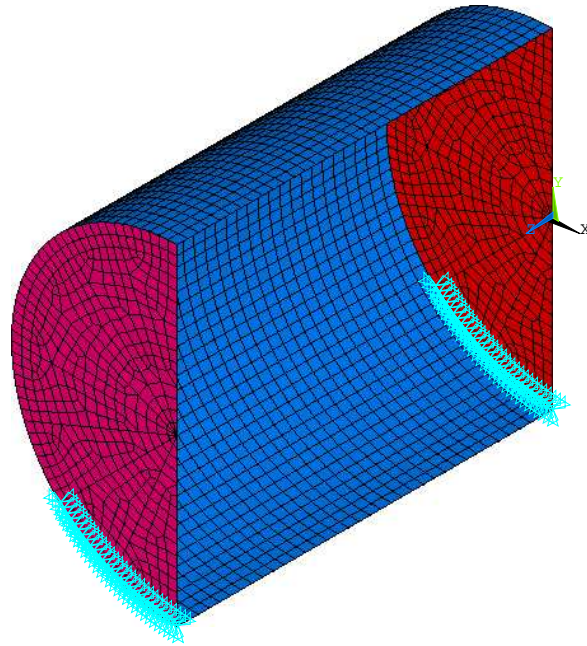


FIG. 2.7: ANSYS model of the Boeing cylinder, showing a cross section through the structure.

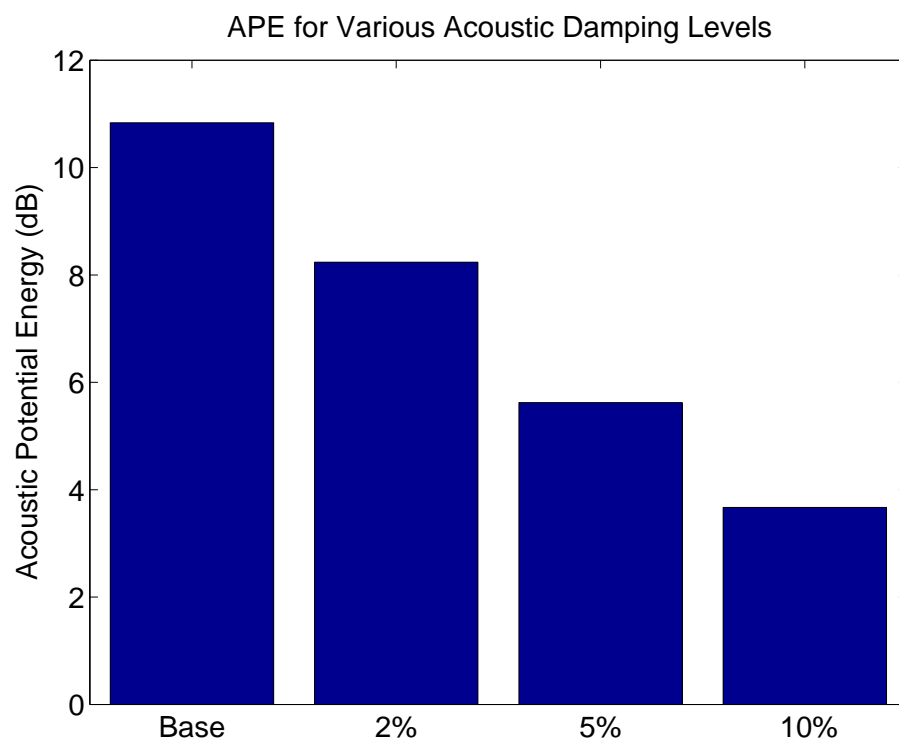


FIG. 2.8: Average APE within the cylinder without PVADs (base), with 20 PVADs arranged into 5 rings with 4 PVADs per ring for various acoustic damping values (loss factors) inside the cylinder.

2.4.2 Stage 3, Task 2

In the original proposal the work statement for this task was as follows:

1. *Address any unexpected issues raised in the Stage 3A work*
2. *Investigate the Feasibility of Stage 4 Tasks*

The tasks that were written in the original contract were intentionally vague, because it was impossible to predict what problems might have occurred in Stage 3, Task 1.

1. The details of the tasks to be investigated in Stage 3, Task 2 were tabulated in the conclusions of Stage 3, Task 1 [4, p73] and are as follows:

- investigate the implementation of a symmetric matrix formulation for the modal coupling method. Symmetric matrices are faster to invert than non-symmetric matrices, and hence the response of the vibro-acoustic system will be evaluated faster than currently.
- investigate the implementation of pseudo-static correction factors to account for modes outside the analysis frequency range.
- compare the integer and binary representations of the chromosomes and determine which method converges to the optimum solution the fastest.
- Preliminary work will be undertaken on Stage 4 tasks 2, 3 and 4 with a view to confirming the feasibility of the proposed approach and investigating the possibility of using alternative approaches to the absorber design and evaluation tasks, which may be preferable to the approach proposed initially.

The major outcomes from this task are listed below.

- Work was done to investigate symmetric matrix formulations for modal coupling. It was found that there is a decrease in the calculation time using this formulation, compared to the formulation using non-symmetric matrices. It was

pointed out that further work was required to extend this to the fully coupled models incorporating Helmholtz resonators and Tuned Mass Dampers.

- Investigations were conducted with pseudo-static correction factors for structural models. The mathematical framework required knowledge of the full mass and stiffness matrices in order to calculate the correction factor. While it is possible to do this for the current method, it was decided that it was unlikely to yield significant benefits in terms of reducing the time for calculations.
- The asynchronous parallel genetic algorithm developed in Stage 3A was reformulated to use integer representations for the chromosomes. The results showed that the optimisations achieved the same reductions in acoustic potential energy with half the number of cost function evaluations compared to using a binary representation for the chromosomes. Thus the integer representation was retained for all future work.
- The feasibility of the work to be undertaken in Stage 4 was investigated:
 - The mathematical framework for the multi-degree of freedom absorbers commenced in Stage 3, Task 1 was shown to be feasible for completing the proposed work in Stage 4.
 - Investigations were conducted to confirm that the FEA software could be used successfully model practical phenomena, such as vent holes and structural stiffeners. The modal coupling theory and the FEA tools that were developed were also amenable to modelling the effect of a rigid or flexible payload inside the fairing.
- A planned task for Stage 4, Task 4 was to incorporate measured data into the modelling and design tools. It was found that whilst this was technically quite feasible, the practical aspects of obtaining good quality data and documentation would make completion of this task unlikely. Instead, it was proposed that in-

vestigations should be conducted into the affect of various acoustic loading conditions on the noise levels inside the fairing and the sensitivity of the optimal configuration of the PVADs to the acoustic loading condition.

- The outcomes of this research were presented at the Australian Acoustic Society 2005 conference (see Howard et al. [16]), at the 12th International Congress of Sound and Vibration (see Howard et al. [17]).

2.5 Stage 4

2.5.1 Stage 4, Task 1: RSLVF optimal and sub-optimal performance evaluation

In the original proposal the work statement for this task was as follows:

The design tools developed in stage 3 will be applied to the Representative Scale Launch Vehicle Fairing (RSLVF) model. The reduction of interior noise levels shall be investigated for different design approaches for the RSLVF. Performance of the tools shall be assessed. The investigation shall include the performance of VADs, which represent vibration and acoustic absorbers at the same location, and the possible benefit of separating them shall be investigated.

The major outcomes from this task are described below.

- It was suggested in Stage 3b that the speed of calculations could be reduced by re-formulating the vibro-acoustic problem by using symmetric matrices and reducing the number of matrix multiplications in the calculation process. This was done as part of this task and resulted in reducing the calculation time by a factor of 2.5 compared to the method used in the previous stages.
- The most significant finding from this stage, and perhaps from the entire project, was the demonstration of the change in the vibro-acoustic response with increasing numbers of absorbers attached to the fairing walls. When there are a few absorbers attached to the structure, the optimal configuration acts to reduce the vibration amplitude of individual vibration modes. However when there are large numbers of absorbers attached to the walls of the fairing, the optimal configuration tends to 'smear' the acoustic energy over a range of frequencies, as shown in Figure 2.9.
- The optimum configuration of absorbers for large numbers of absorbers attached to the fairing walls had a continuous distribution of the resonance frequencies for both the acoustic and vibration absorbers, as shown in Figure 2.10. It was thought that the optimal configuration of the absorbers might have resulted in

‘clusters’ of resonance frequencies that corresponded to particular acoustic or vibration modes. However this was not the case and the optimal configuration is for both the acoustic and vibration absorbers to have a continuous distribution of resonance frequencies.

- The optimal configuration for the damping for the absorbers did not indicate any identifiable trends, compared with the results for the resonance frequencies. Figure 2.11 shows the damping factors for the acoustic and vibration absorbers and there appears to be an even distribution of damping factors across all frequency ranges.
- Analyses were conducted to compare the noise reduction when using acoustic and vibration absorbers combined into a single dual-purpose absorber, and when the locations of the acoustic and vibration absorbers were separated [6, p68]. The results showed that there was only a 0.5dB improvement, which was not considered to be significant.
- There were two results that were not included in the report for Stage 4, Task 1 that were published in Howard et al. [18] and it is worth summarising these results here. Investigations were conducted to determine the ‘sensitivity’ of the location of the PVADs to changes in the total acoustic potential energy. The optimum solutions for the 10 and 500 PVADs cases were further analysed by investigating whether changes in the location of the PVADs would cause significant changes in the APE. The locations of each of the PVADs was randomly altered to another nearby location in a circular selection zone and the APE was recalculated. This random selection process was completed ten times for each radius so that the range of APE could be investigated. The radius of the selection zone was varied as 0.0m, 0.08m, 0.1m 0.2m, and 0.4m. Figure 2.12 shows the variation in the acoustic potential energy with the change in the radius of the selection zone for the 10 and 500 PVADs cases. The optimal result obtained from the GA optimi-

sations of 10 TMDs is shown as the solid line at -15.1dB, and the optimum for the 500 PVADs case is shown as the solid line at -20.3dB. Examination of these two results shows that as expected the use of 500 absorbers is less sensitive to changes in their placement than the results for 10 absorbers. Similarly, it is likely that the use of 500 absorbers is less sensitive to variations in the external acoustic excitation of the fairing than the use of 10 absorbers.

- Figure 2.13 shows the decrease in the total acoustic potential energy with increasing number of PVADs, with a logarithmic scale for the number of PVADs. The results show that there is a limit to the improvement in noise reduction that can be achieved by increasing the number of PVADs for the same added mass. These results show that the greatest noise reduction is obtained for the largest number of lightweight dampers.
- Another result that was not included in the Stage 4, Task 1 report was an analysis to determine the benefit of having a vibrating mass for the TMD compared to having a lumped mass, also termed a 'blocking-mass' in some research literature [19]. The circle markers in Figure 2.13 show the APE with the optimum parameters for the PVADs, but with the stiffness of the TMDs so large that it effectively created a rigid-mass attached to the RSLVF walls. The results show that there is a significant difference between the use of a TMD and a rigid mass.
- The outcomes of this research were published in the Applied Acoustics journal (see Howard et al. [18]).

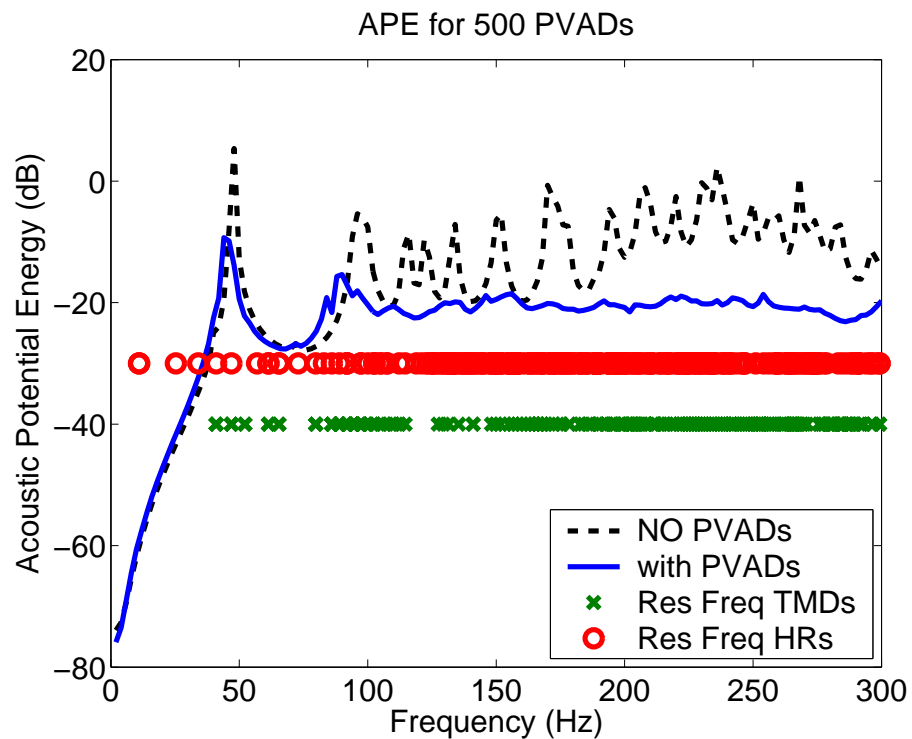


FIG. 2.9: Acoustic potential energy versus frequency for 500 PVADs attached to the walls of the RSLVF fairing.

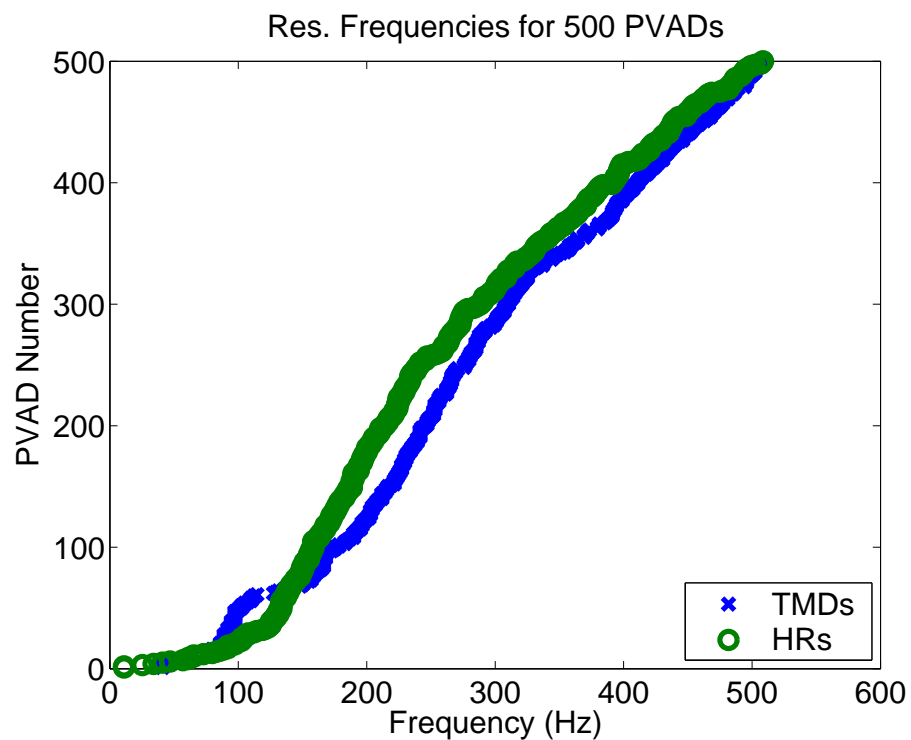


FIG. 2.10: Resonance frequencies for 500 PVADs corresponding to the results shown in Figure 2.9.

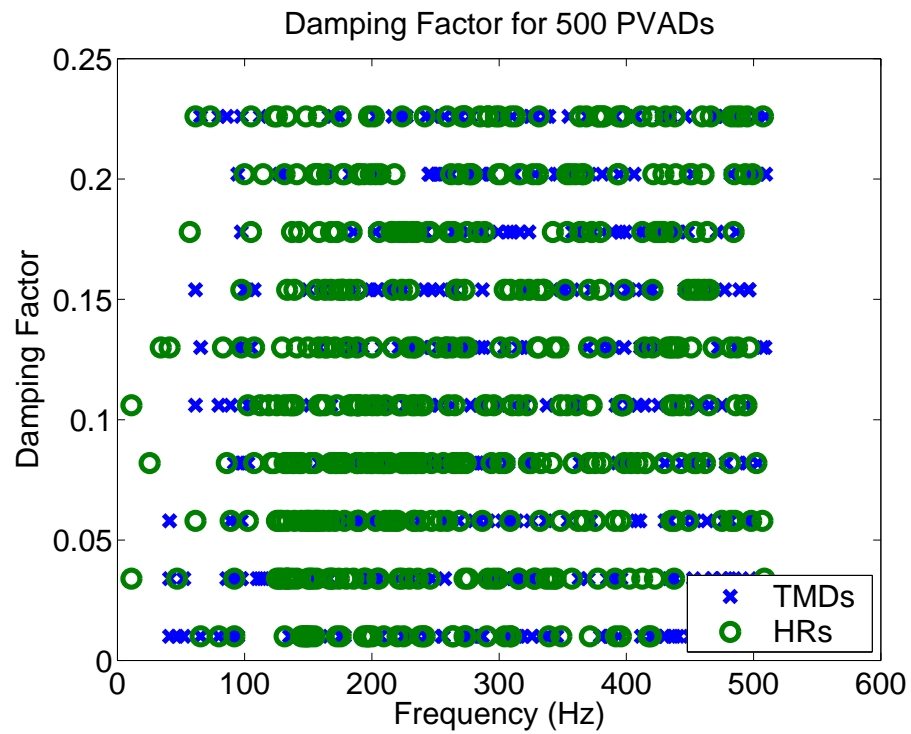


FIG. 2.11: Damping factor versus frequency for 500 PVADs.

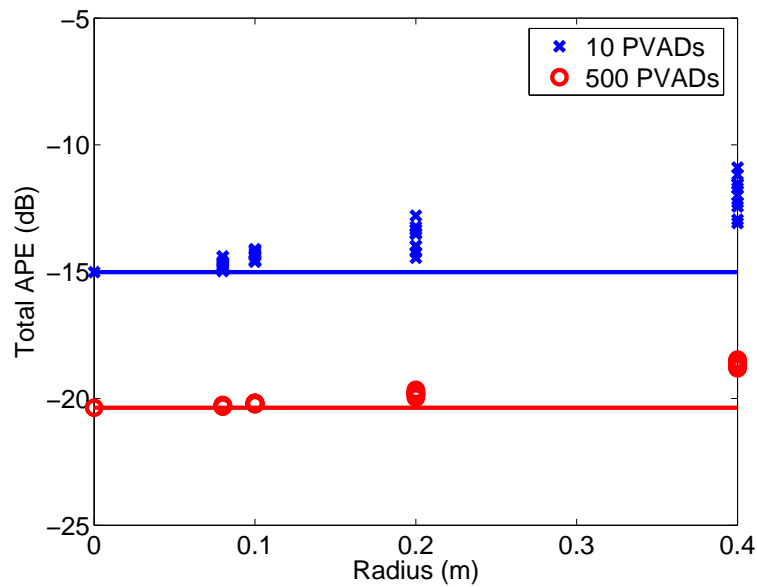


FIG. 2.12: Acoustic potential energy versus the radius for the selection zone, for 10 and 500 PVADs.

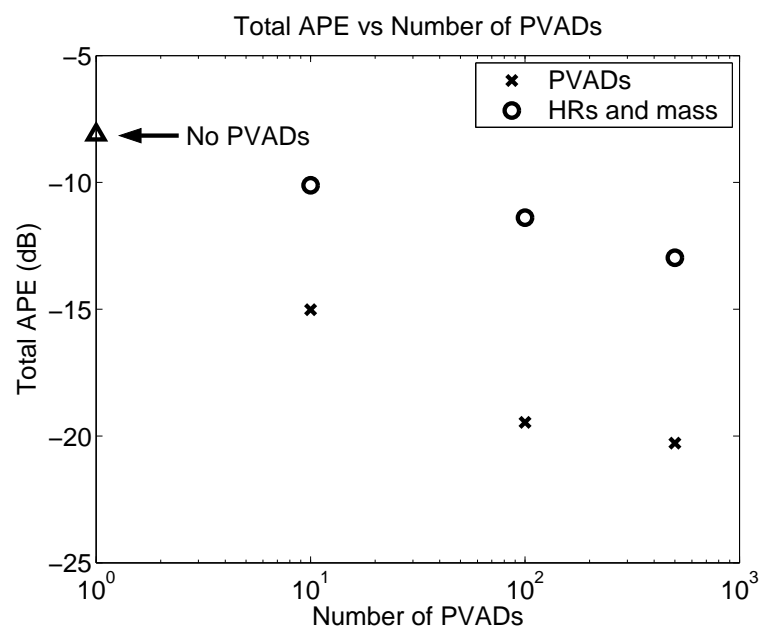


FIG. 2.13: Acoustic potential energy versus the number of PVADs.

2.5.2 Stage 4, Task 2: Optimal design of multiple degree of freedom vibro-acoustic dampers

In the original proposal the work statement for this task was as follows:

The design of a multi-degree-of-freedom vibro-acoustic absorber with rocking modes and a twisting mode in addition to the normal translational modes will be investigated. Key design issues shall be identified and design techniques developed.

The major outcomes from this task are described below.

- A theoretical framework for the application of multiple degree of freedom dampers attached to the vibrating fairing was developed [6, p74]. The type of absorber that was investigated was a tuned-mass-damper that had 4 cantilevered arms. A finite element model of this type of absorber is shown in Figure 2.14. This absorber was capable of transmitting both translational forces and rotational moments to the structure.
- The results from the optimisation with the multiple degree of freedom tuned mass dampers showed that the same amount of noise reduction could be achieved using 20 multiple DOF PVADs as using 500 single-DOF PVADs, as shown in Figure 2.15. In addition, the noise-reduction in the low frequency range using the absorbers with both translational and rotational degrees-of-freedom was significantly greater than using the absorbers with only translational degrees-of-freedom, as shown in Figure 2.16.
- The outcomes of this research were presented at the Australian Acoustic Society conference and a paper was published in the conference proceedings (see Howard et al. [20]).

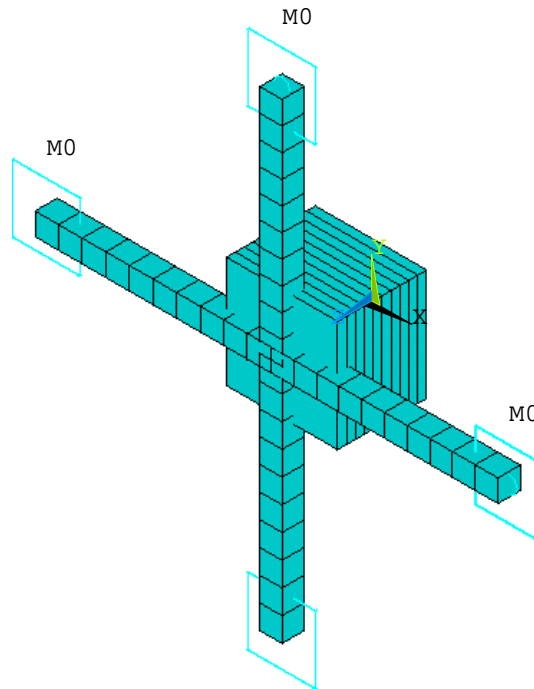


FIG. 2.14: ANSYS model of the 4 cantilevered arms with masses on the ends.

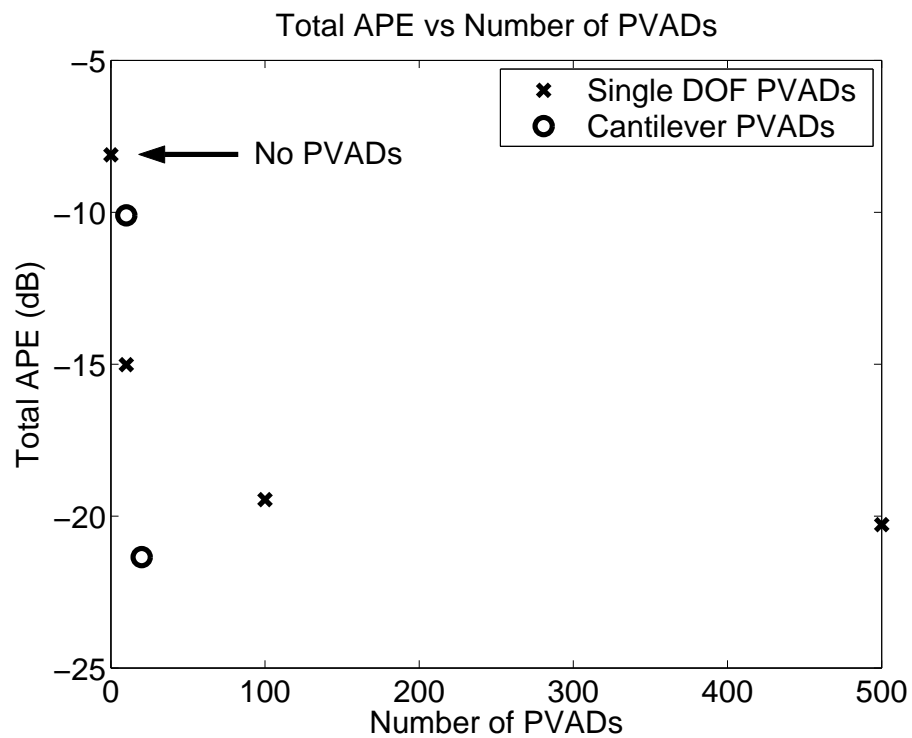


FIG. 2.15: Comparison of the total APE versus the number of PVADs for the single degree of freedom PVADs and the cantilever PVADs with 3 degrees of freedom.

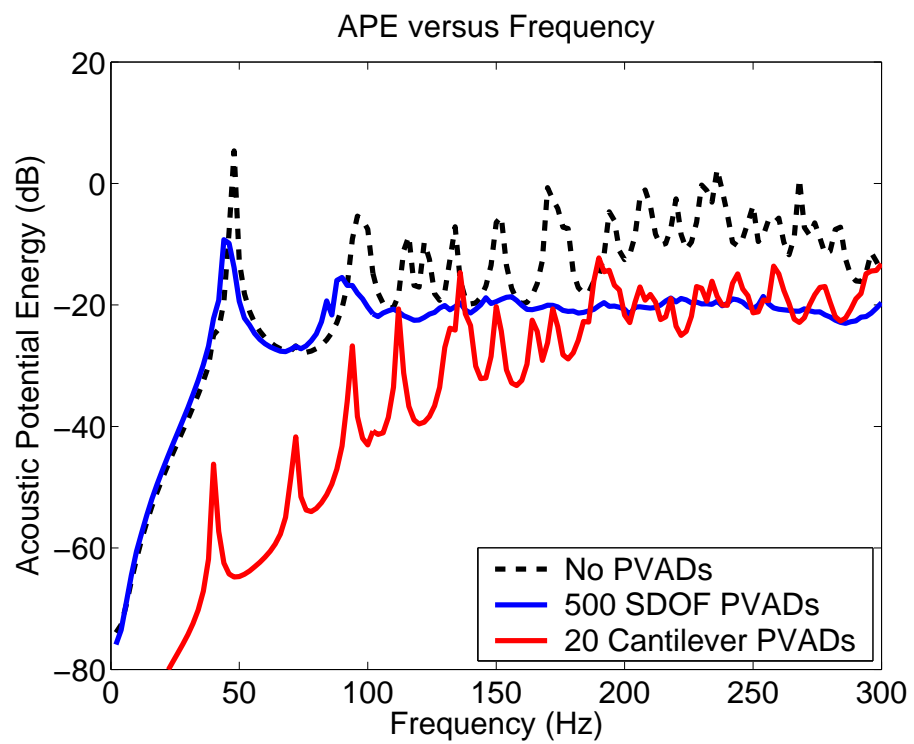


FIG. 2.16: Acoustic potential energy versus frequency for no PVADs, 500 single degree of freedom PVADs, and 20 cantilever PVADs.

2.5.3 Stage 4, Task 3: Incorporation of Practical Phenomena into the Modeling and Design Process

In the original proposal the work statement for this task was as follows:

Having developed efficient computation methods in Task 4.1, and having developed improved PVAD devices in Task 4.2, the contractor shall study the effects of the following practical phenomena:

- *structural anomalies - including a vent, a separation seam, and /or a variation in the boundary conditions, and*
- *Acoustic fill - including the determination of the effect of having a rigid payload and a resonant payload in the interior volume.*

The major outcomes from this task are described below.

- An analysis of the RSLVF with vent holes showed that there was no appreciable difference in the modal response of the acoustic cavity. Consequently, there was no difference in the results for the optimisation of absorbers attached to the fairing [7, p13].
- An analysis was undertaken of the RSLVF with a separation seam along the length of the fairing, which was modelled as an aluminium beam of dimensions 100mm × 3mm, with the beam orientated to provide the greatest increase in stiffness to the fairing, as shown in Figure 2.17. The modal analysis of the fairing with the separation seam slightly altered the modal response of the structure compared to the unmodified fairing. However, there was no appreciable difference in the acoustic potential energy with the separation and the unmodified fairing [7, p17].
- An analysis was undertaken of the effect of payload 'fill' on the noise levels inside the fairing [7, p18]. Previous researchers have predicted using Statistical

Energy Analysis methods that there should be an increase in noise levels due to the presence of a payload. Analyses were conducted to determine the increase in the acoustic potential energy levels inside the payload bay for three sizes of rigid payloads, and three sizes of flexible payloads. An example of one of the payload sizes is shown in Figure 2.18. There were surprising results from this investigation and have these been explained further after this summary of results for Task 3 of Stage 4.

- It was shown that the presence of a rigid or flexible payload increased the sound pressure level within the fairing, to a greater extent than predicted using methods developed at NASA using Statistical Energy Analysis (SEA) [7, p33]. The comparative increase in SPL due the presence of a rigid payload is shown in Figure 2.19. The reasons for the differences between the results presented here and the NASA predictions could be due the assumptions used in the NASA model. The NASA model does not take into account the acoustic loading conditions. In addition, it is assumed that the modal energy of the interior space is not altered by the presence of the payload, so that the ratio of the filled to empty modal energies can be set to one. The modal densities of the empty and filled space are then calculated in terms of the volume of the space and the gap distance between the payload and the fairing wall [21]. However, the presence of the payload in the fairing alters the acoustic modal response of the system, and hence it is possible that the modal densities, and hence modal energies, of the empty and filled payloads will differ, which might explain why the results calculated using FEA and presented here differ from the NASA predictions that used SEA. Another possible explanation for the difference in results is that the modal coupling method used in this project does not account for 'radiation damping', where the structure re-radiates sound from the reverberant field in the payload bay to the exterior. If this were included in the model, it would follow that the sound pressure level in the payload bay would be lower than if radiation damping had not been in-

cluded. However it is expected that this would only be a small effect.

- It was shown that better noise reduction was obtained when 100 PVADs were optimised for each particular payload fill, compared to optimising the PVADs for the empty configuration. Figures 2.20 and 2.21 show the improvement in noise reduction for optimising the payload for each configuration with a rigid payload, and flexible payload, respectively.

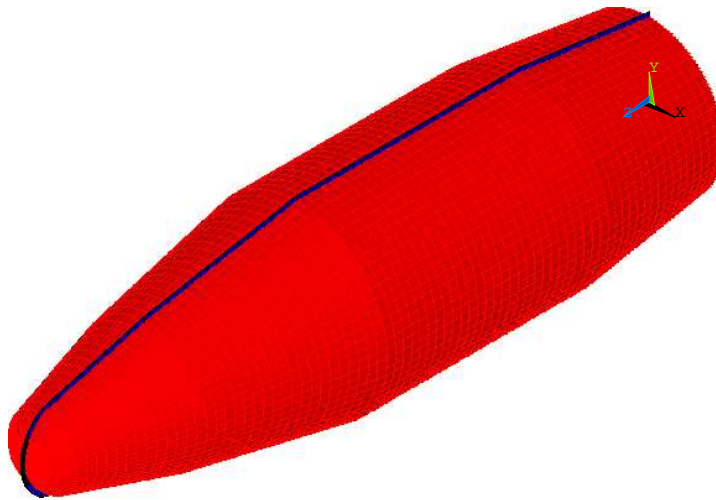


FIG. 2.17: Finite element model of the RSLVF showing the stiffeners for the separation seam.

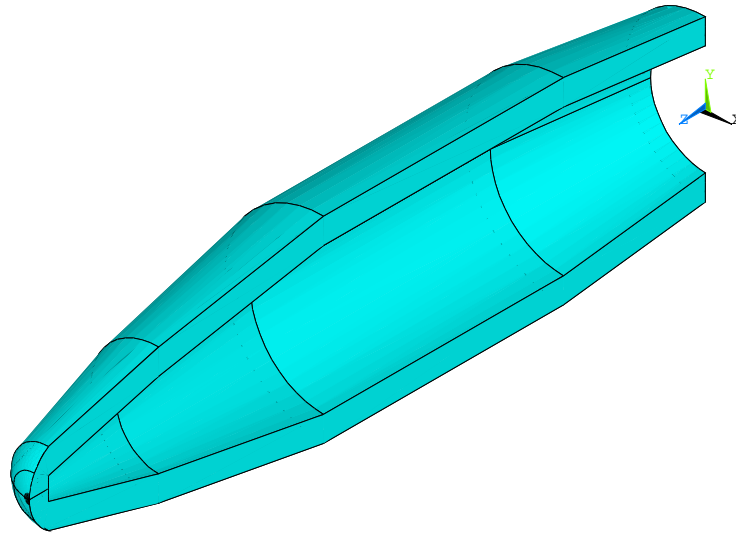


FIG. 2.18: Cross sectional view of the solid model of the RSLVF showing a hole for rigid payload that has a similar profile as the RSLVF, with a gap distance of 0.2m.

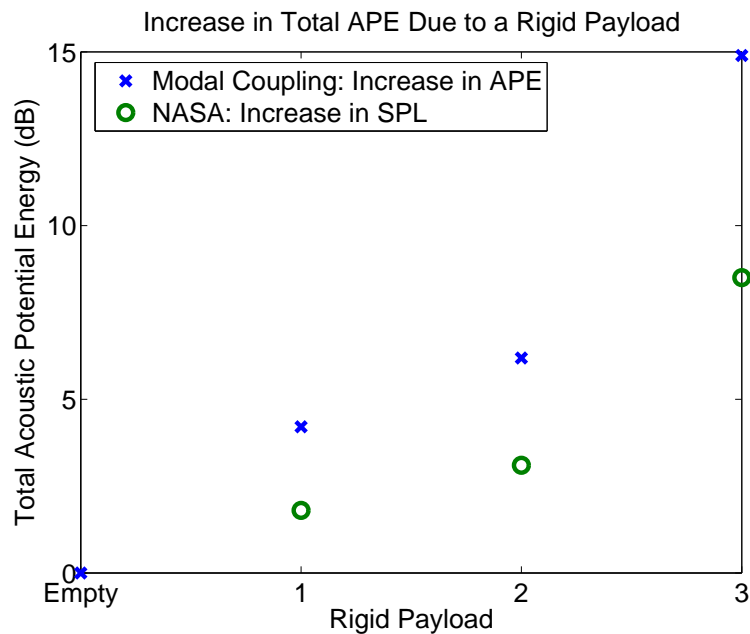


FIG. 2.19: Increase in total APE (over the frequency range 0-300Hz) for the RSLVF with an empty fairing, and rigid payloads 1, 2, 3 for an incident pressure wave of 60deg inclination compared with the NASA predictions.

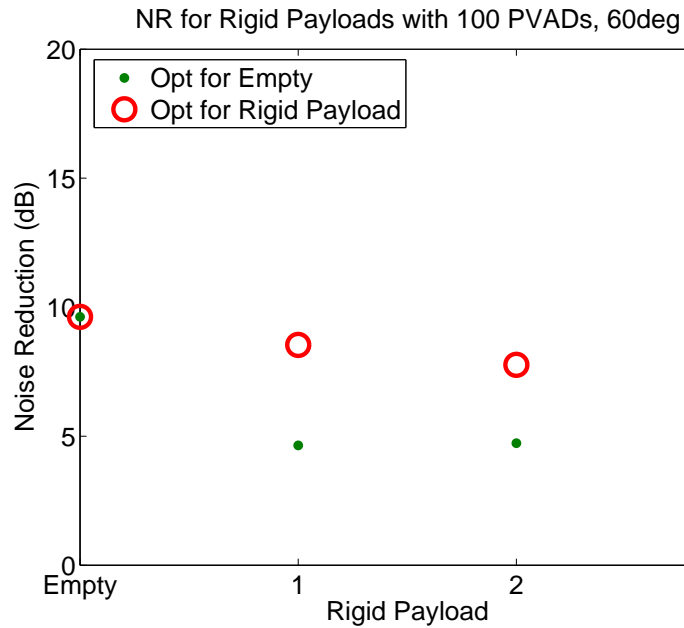


FIG. 2.20: Noise reduction for an empty fairing and rigid payloads 1, 2, 3 in terms of the total APE (over the frequency range 0-300Hz) with 100 PVADs optimised for each payload configuration.

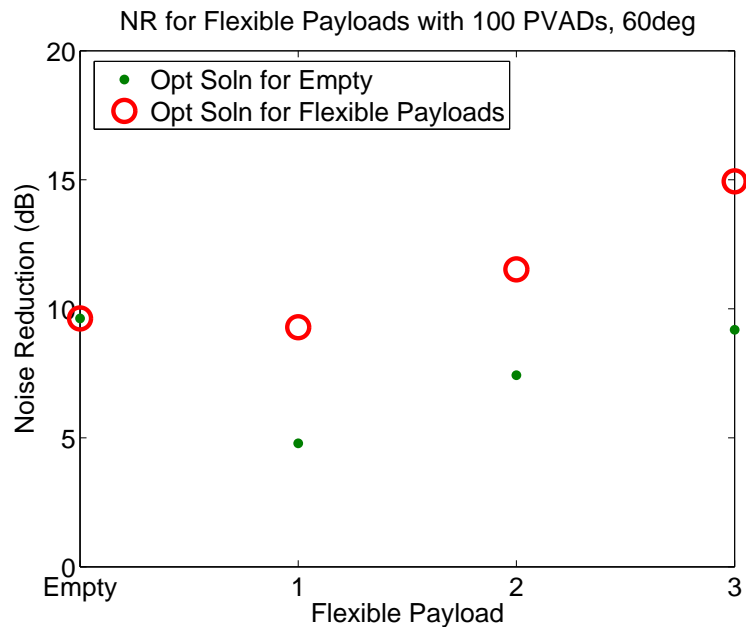


FIG. 2.21: Noise reduction for the RSLVF for a plane incident pressure wave of 60degrees inclination with PVADs optimised for the empty fairing, and optimised for the particular flexible payload configuration.

Effect of Payload Fill

Koganei et al. [22] used boundary element methods to examine the influence of the increase in the interior sound pressure level due to the presence of a payload in the bay of a launch vehicle. They conducted analyses that involved varying the gap distance between the payload and the payload bay walls. Their theoretical modelling showed that there was an increase in the sound pressure level at frequencies that were related the gap distance. This is intuitively what most acousticians would predict.

However, the results from the investigations conducted in Stage 4, Task 3 [7, p31] show that the first acoustic resonance frequency decreases when the gap between the payload and the fairing wall decreases. The implication for this result is that as the gap distance becomes smaller, the sound pressure level will increase at the lowest resonance frequency, shifting more acoustic energy into lower frequencies. This characteristic was explained using an analogy of a Helmholtz resonator.

The acoustic space within the fairing has a thin acoustic-cavity between the outer-walls of the fairing and the payload. On top of the thin acoustic-cavity is the volume for the nose cone. The interaction of these components is important for the overall resonance behaviour of the system. An analogy can be made between this system and a Helmholtz resonator, where the volume of fluid between the fairing walls and the payload can be thought of as a compliant spring, and the volume of fluid within the nose cone can be thought of as an acoustic mass. The simplified expressions for the stiffness k of the acoustic volume, the equivalent mass m , and the resonance frequency f for a Helmholtz resonator are given approximately by [23]:

$$k = \frac{\rho c^2 A_{\text{neck}}^2}{V_{\text{HR}}} \quad (2.1)$$

$$m = \rho A_{\text{neck}} L_{\text{eff}} \quad (2.2)$$

$$f = \frac{c}{2\pi} \sqrt{\frac{A_{\text{neck}}}{L_{\text{eff}} V_{\text{HR}}}} \quad (2.3)$$

where f is the resonance frequency of the Helmholtz in Hz, ρ is the density of the fluid, c is the speed of sound, A_{neck} is the cross-sectional area of the throat, L_{eff} is the effective length of the neck, and V_{HR} is the volume of the compliant fluid. If the analogy of the Helmholtz resonator with the system shown in Figure 2.22 is used, the expressions for the stiffness, mass and resonance frequency are

$$k = \frac{\rho c^2 A_{\text{neck}}^2}{A_{\text{neck}} L_1} \quad (2.4)$$

$$m = \rho L_2 \pi (\text{OD})^2 / 4 \quad (2.5)$$

$$f = \frac{c}{\pi (\text{OD})} \sqrt{\frac{A_{\text{neck}}}{\pi L_1 L_2}} \quad (2.6)$$

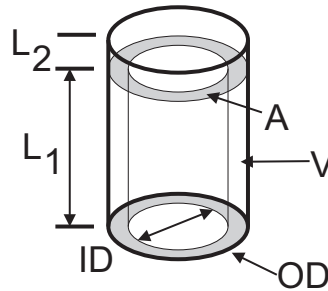


FIG. 2.22: Diagram of a hollow cylinder with end cap that was modelled using finite element analysis.

For the analyses conducted in Stage 4 Task 3, as the payload volume increases (ID increases), the cross sectional area A decreases, and the lengths L_1 and L_2 remain constant. Hence, from the simplified expression for the resonance frequency of a cylinder with an end-cap shown in Eq. (2.6), one could expect that the resonance frequency would decrease as the cross sectional area A_{neck} decreases.

Thus, for the case of the RSLVF, as the size of the payload increases to fill the entire volume of the payload bay, the cross sectional area between the walls and the payload becomes smaller and the first acoustic resonance frequency of the cavity will decrease. The implication is that the acoustic energy will be shifted into lower frequencies, where it is more difficult to attenuate noise using conventional noise control treatment. This

result is the opposite of that found by Koganei et al. [22].

2.5.4 Stage 4, Task 4: Sensitivity of Results to Various Acoustic Loading Conditions

In the original proposal the work statement for this task was as follows:

Task 4.4: Sensitivity of results to various acoustic loading conditions

The contractor shall examine the sensitivity of the acoustic performance to several acoustic loading conditions such as perpendicular plane harmonic waves, oblique plane harmonic waves, and oblique plane waves with random phase that strike the circumference of the rocket fairing and determine the optimal configuration of VADs for best performance.

In the past, a number of researchers have attempted to create mathematical models of the acoustic field that impinges on a launch vehicle fairing during launch. The purpose of creating acoustic models of the launch environment is to use them to estimate the loading conditions for vibro-acoustic models of the fairing and payload. Researchers have modelled the sound field that strikes the fairing as harmonic waves incident at oblique angles [19, 24–26] as well as an incident reverberant field [9, 27–30].

A significant amount of work has been undertaken by aerospace companies to develop “acoustic blankets” or similar passive noise reduction devices to reduce the noise levels inside the payload bay of launch vehicles. Some researchers consider that the noise control treatment that is applied to the fairing should be optimised for a particular directivity of the noise source [31], which makes sense if the direction of the exhaust plume is known. Other researchers attempt to create a distributed noise control treatment so that the noise reduction that is achieved is independent of the direction of the acoustic source relative to the fairing orientation; for example Ref [32].

The work reported in Stage 4, Task 4 is focused on an examination of acoustic loading conditions on the noise levels inside the fairing for the two cases of harmonic acoustic waves and acoustic waves of random phase arriving at an oblique angle to the fairing axis.

The major outcomes from this task are described below.

- A mathematical model described by Potter [24] for the acoustic loading of harmonic plane waves incident on a cylinder at an oblique angle was adapted for use with a complex shaped object such as the RSLVF examined in this task [7, p60]. The acoustic loading used in this task did not include diffraction effects, but did include the shadow effect where surfaces that were hidden from the acoustic source by another surface, were not excited with the acoustic pressure loading.
- Optimisations of the PVADs were conducted for the following configurations of acoustic loading:
 - no PVADs attached to the fairing for acoustic loads from several angles of incidence,
 - 100 PVADs attached to the fairing that have been optimised for acoustic loading at a 60 degree angle of inclination and applied to the fairing with various angles of incidence of the acoustic loading,
 - 100 PVADs attached to the fairing that have been optimised for the acoustic loading from the particular angle of inclination.

Figure 2.23 shows a summary of the total acoustic potential energy when harmonic plane waves struck the fairing for the optimisation of 100 PVADs for the configurations described above, and Figure 2.24 shows the corresponding noise reduction. The results show that the best noise reduction is obtained when the PVADs are optimised for the particular angle of incidence of the acoustic loading.

- Similar analyses were conducted for acoustic waves characterised by random phase [7, p73]. Figure 2.25 shows a summary of the results in terms of the total acoustic potential energy for the various optimisation approaches considered for acoustic loading with random phase. Figure 2.26 shows the same data in terms of the reduction in the total acoustic potential energy over the frequency range

0-300Hz, for the optimisation of 100 PVADs attached to the fairing for acoustic loading with random phase. The results show that the greatest noise reduction is achieved when the PVADs are optimised for the particular angle of incidence of the acoustic loading. The improvement obtained by optimising for the actual angle of incidence, compared to optimising for 60 degrees incidence, ranges from 2-4dB out of a maximum achievable 10dB.

- Figure 2.27 shows the noise reduction, in terms of the total acoustic potential energy over the frequency range 0-300Hz, for 100 PVADs attached to the fairing that have been optimised for the particular angle of incidence of the acoustic loading, for acoustic loading characterised by harmonic plane waves and acoustic waves with random phase. The results show that there is about 10dB reduction in the total acoustic potential energy for the two types of acoustic loading is achievable and that the achievable reduction is relatively independent of the type of acoustic loading.
- The results for the distribution of the optimum locations of the PVADs for the harmonic plane waves and acoustic waves with random phase show that the optimum locations for the PVADs cluster around 0 and 180 degrees. However, comparison of the optimum locations for a particular angle of incidence for harmonic plane waves and acoustic waves with random phase, shows that the distributions are dissimilar. This result highlights that the optimum location of the PVADs is dependent on the type of the acoustic load on the fairing: harmonic plane waves, or acoustic waves with random phase, or in between where there is a spatial phase correlation relationship of the acoustic source. However, either distribution of PVADs provides good noise reduction. This finding supports the conclusions of Stage 4B, where it was found that when a large number of PVADs were attached to the fairing (> 100) the noise reduction was relatively insensitive to the location of the PVADs compared to the use of a few PVADs (about 10).

- The greatest benefit of the noise control treatment is obtained when the PVADs are optimised for a specific angle of incidence and acoustic wave type.
- Figure 2.28 shows the total acoustic potential energy inside the fairing for varying angles of incidence of the acoustic loading which is characterised by random phase for three cases:
 1. when no PVADs were attached to the fairing,
 2. when 100 PVADs were attached to the RSLVF that had been **optimised for harmonic acoustic loads** at angles of incidence of 0, 20, 40, 60, and 80 degrees and subjected to acoustic waves with random phase at angles of incidence of 0, 20, 40, 60, and 80 degrees respectively, and
 3. when 100 PVADs were attached to the RSLVF that had been **optimised for acoustic waves with random phase** at angles of incidence of 0, 20, 40, 60, and 80 degrees and subjected to acoustic waves with random phase at angles of incidence of 0, 20, 40, 60, and 80 degrees respectively.

The results show that there is little degradation in performance when the 100 PVADs that were optimised for harmonic loads were applied to the RSLVF and subjected to acoustic waves characterised by random phase.

- Figure 2.29 shows the noise reduction data shown in Figure 2.27 and the additional data for the noise reduction for 100 PVADs attached to the fairing that have been optimised for the particular angle of incidence of acoustic loading characterised by harmonic plane waves, when the RSLVF was subjected to acoustic waves with random phase, and shown as the green plus sign. The results in this figure indicate that in general it is best to optimise the noise control treatment for the acoustic loading conditions, however at some angles of incidence there was no degradation in noise reduction when the 100 PVADs that were optimised for harmonic acoustic loads were attached to the RSLVF and subjected to acoustic waves characterised by random phase.

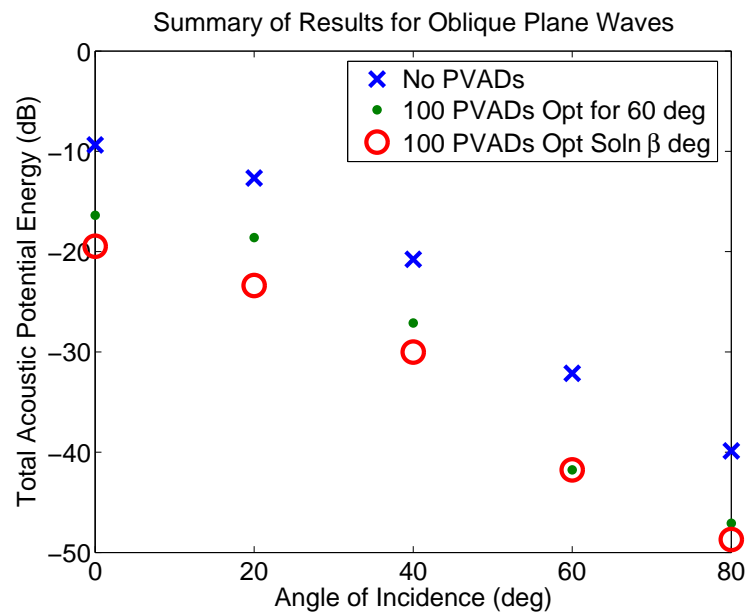


FIG. 2.23: Summary of the total acoustic potential energy results for the optimisation of 100 PVADs for harmonic loading.

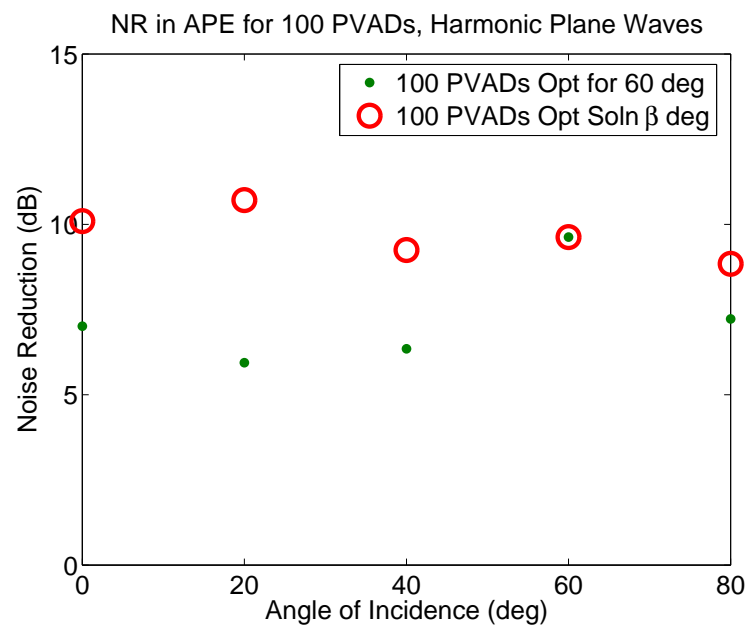


FIG. 2.24: Noise reduction for 100 PVADs for various incident angles of the incoming harmonic sound.

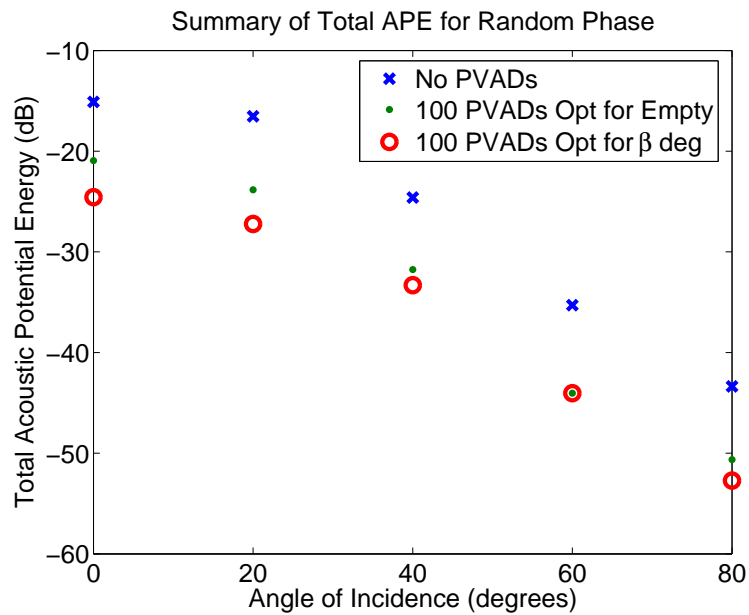


FIG. 2.25: Summary of the total APE (over the frequency range 0-300Hz) for optimisation of the PVADs for the random phase acoustic loading.

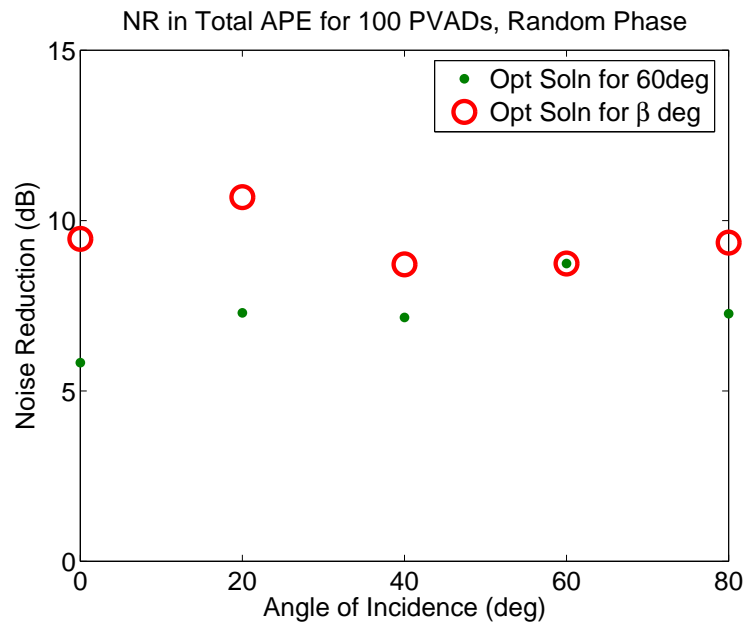


FIG. 2.26: Noise reduction in terms of total APE (over the frequency range 0-300Hz) for optimisation of the PVADs for the random phase acoustic loading.

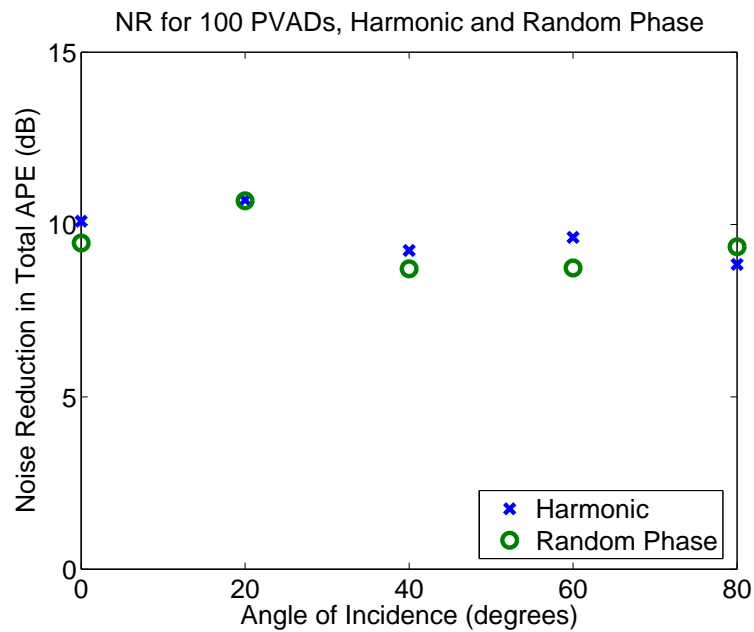


FIG. 2.27: Noise reduction in terms of total APE (over the frequency range 0-300Hz) for optimisation of the PVADs for the random phase acoustic loading.

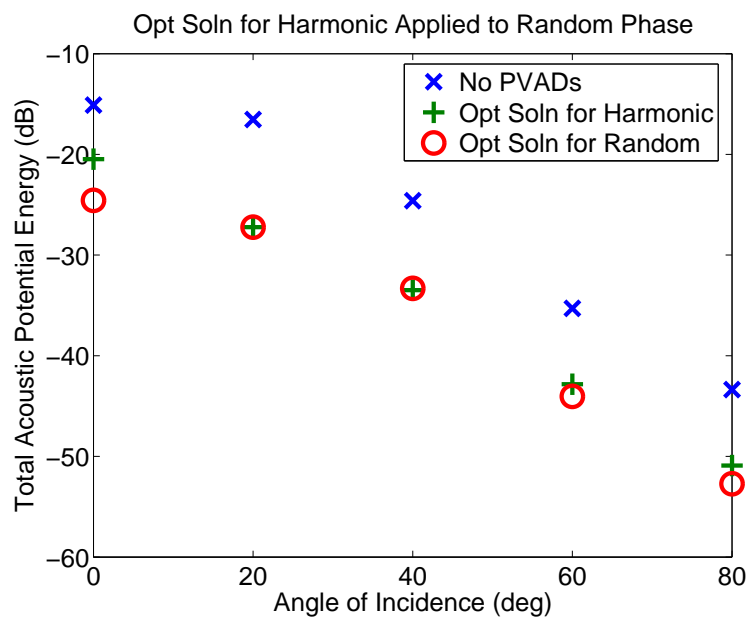


FIG. 2.28: Noise reduction in terms of total APE (over the frequency range 0-300Hz) for optimisation of the PVADs for the random phase acoustic loading.

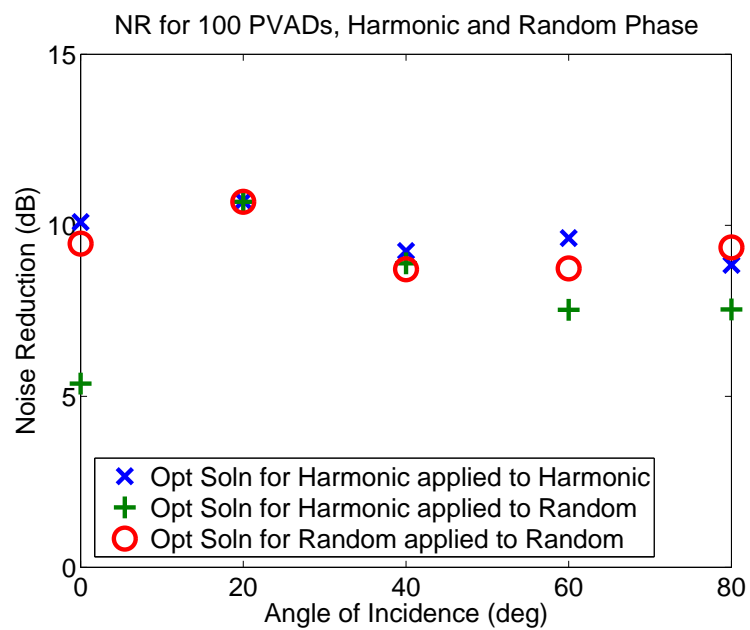


FIG. 2.29: Noise reduction in terms of total APE (over the frequency range 0-300Hz) for optimisation of the PVADs for the random phase acoustic loading.

Chapter 3

Conclusions

3.1 Major Outcomes

The major outcomes from this project were:

- Development of a mathematical model in Matlab that can be used to predict the sound pressure level inside an enclosed volume of any shape [3, p10], [4, p12].
- Development of a 'super-computer', by utilising unused desktop computers in student computing laboratories, to conduct the vibro-acoustic optimisation in this project [4, p31].
- Development of a semi-synchronous parallel genetic algorithm for the optimisation of the locations and configurations of acoustic and vibration absorbers attached to a vibro-acoustic system [4, p31].
- A demonstration that that the greatest transmission loss for a given 'mass budget' was obtained when the mass was 'used' in the form of combined tuned vibration absorbers that had a continuous distribution of resonance frequencies. This has the effect of 'smearing' the acoustic energy absorption over a range of frequencies.
- The development and analysis of tuned mass dampers that have both transla-

tional and rotational degrees of freedom, and a demonstration that these dampers can significantly reduce the structural vibration and hence the noise levels transmitted into the launch vehicle fairing work.

3.2 Recommendations for Future Work

The results from the research that has been conducted in this project has shown that the greatest reduction in noise levels inside the payload bay can be achieved by using:

- a large number of lightweight tuned vibration absorbers
- tuned vibration absorbers that have both translational and rotational degrees of freedom
- Helmholtz resonators and tuned vibration absorbers that have a continuous distribution of resonance frequencies
- high levels of acoustic damping within the fairing

Further work is required to:

- implement vibration control using tuned mass absorbers that specifically use the rotational degree of freedom to alter the vibration response of the structure;
- demonstrate experimentally the theoretical concepts that were developed as part of this project; and
- create compact acoustic absorbers that have a continuous distribution of resonance frequencies.

The work conducted in Stages 1 to 4 involved the development of mathematical models and implementation of the models in software. Although the contract did not specifically require the contractors to conduct experiments, it is the opinion of the author that experimental testing would *indicate* the validity of the theoretical models that

were developed in this multi-stage project. Some preliminary experimental work has been conducted to demonstrate some of the concepts proposed in this project, and the preliminary results are presented in Appendix A.

The creation of acoustic absorbers for use in a rocket fairing has been partially completed with the ChamberCore design for composite fairings [33], which targeted the reduction of the first four acoustic modes in the fairing. The work proposed here differs from the ChamberCore design and involves the development of broad-band acoustic absorbers as part of the fairing structure that would provide high levels of acoustic damping at low frequencies. The problem with most acoustic damping treatments is that they are only become effective at mid-frequencies, above 400Hz, and the work proposed here aims to address this problem.

The proposed acoustic treatment could be constructed within the double-walls of a fairing structure for a rocket launch vehicle, or an aircraft. It would not occupy any volume within the payload area, and not add any significant weight, if it were constructed as part of the fuselage structure. In addition, the proposed acoustic treatment would attenuate noise across a broad range of frequencies, rather than targeting individual resonant modes of a cavity.

Appendix A

Experimental Testing

A.1 Introduction

This appendix describes an experiment that was designed to examine the increase in transmission loss that could be achieved by adding tuned vibration absorbers to a clamped panel. The appendix contains:

- a theoretical model for the transmission loss of rectangular clamped panel.
- the results of the experimental transmission loss testing of a clamped rectangular panel with and without absorbers.

A.2 Transmission Loss of Panels

The field incidence transmission in the mass-law frequency range, below the critical frequency of a panel $f_c/2$ for isotropic infinite panels is given by (see [34, Eq. (8.27)] or [35, p383, Eq. (13.15.6)])

$$TL = 20 \log_{10} \left[1 + \frac{\pi f \rho_s}{(\rho_0 c)} \right] - 5.5 \text{ (dB)} \quad (\text{A.1})$$

where f is the frequency in Hz, ρ_s is the mass per unit area of the panel, ρ_0 is the density of air, and c is the speed of sound. It can be seen from Eq. (A.1) that there is no term

for the area of the panel, as this equation assumes that the panel is infinite in extent.

The transmission loss for a *finite* panel can be predicted using the method described by Sewell [36], but explained more clearly by Fahy [12, p162, Eq. (4.57)]. The sound reduction index, which is equivalent to sound transmission loss, for non-resonant panels (nr) is given by

$$R_{nr} \approx R(0) - 10 \log_{10}[\ln(kA^{1/2})] + 20 \log_{10}[1 - (\omega/\omega_c)^2] \quad (\text{dB}) \quad (\text{A.2})$$

where A is the area of the panel, c is the speed of sound in air, ω is the frequency in radians / second, $k = \omega/c$ is the wavenumber, ω_c is the critical frequency (or coincidence frequency) of the panel given by [12, p152, Eq. (4.41)]

$$\omega_c = c^2 \sqrt{m/D} \quad (\text{A.3})$$

m is the mass of the panel per unit area ($m = \rho_s h$ where h is the thickness of the panel), D is the bending stiffness calculated as [12, p126]

$$D = \frac{Eh^3}{12(1 - \nu^2)} \quad (\text{A.4})$$

E is the Young's modulus, h is the panel thickness, ν is Poisson's ratio, and $R(0)$ is calculated using the expression [12, p155, Eq. (4.46)]

$$R(\phi) = 20 \log_{10} \left(\frac{\omega m \cos(\phi)}{(2\rho_0 c)} \right) \quad (\text{A.5})$$

with $\phi = 0$ and ρ_0 is the density of air.

A.3 Experimental Testing

A.3.1 Introduction

An experiment was conducted to determine the increase in transmission loss due to having numerous tuned vibration absorbers attached to a rectangular panel. The experiments were conducted in the transmission loss test facilities at the School of Mechanical Engineering, University of Adelaide. The properties of the acoustic chambers are given in Appendix B.

A.3.2 Experimental Setup

An aluminium rectangular panel that has dimensions of $1.0\text{m} \times 1.5\text{m} \times 1.5\text{mm}$ was mounted in a clamped frame between two reverberation chambers. Figure A.1 shows a picture of the experimental setup which was taken from inside the acoustic source room of the transmission loss facility. A pink-noise source of about 100dB was created in the source room using 3 sets of loudspeakers. The average sound pressure levels in the source and receiver rooms were measured using microphone traverse systems. The figure shows a scanning 3D Polytec laser vibrometer that was used to measure the vibration of the rectangular panel. The rectangular panel had 49 cantilever absorbers attached to the panel and a close-up picture of the absorbers attached to the panel is shown in Figure A.2. It should be noted that the absorbers were designed to act only as translational absorbers, and were **not** designed to provide restoring rotational moments to the panel. The absorbers were designed as cantilevers, because this design was considered the easiest to implement. The lengths of both arms on each cantilever was the same to prevent rotational moments being generated by the absorber when vibrating. Experiments were conducted to measure the transmission loss of the aluminium panel without absorbers and with 49 absorbers.



FIG. A.1: Picture of the reverberation chamber showing the scanning Polytec Laser vibrometer and the panel with cantilever strips attached.



FIG. A.2: Picture of the cantilevers attached to the panel.

Figure A.3 shows the predicted and experimentally measured resonance frequencies of the cantilevers. The theoretical values of the resonance frequencies of the cantilevers was calculated using simple beam theory from Young [37]. The resonance frequencies of the cantilevers was experimentally measured by mounting the absorbers to a B&K impedance head that was attached to a Ling Dynamics V103 shaker and the system was orientated so that the axis of the shaker was vertical. The results show that the experimentally measured resonance frequencies were about 5% lower than theoretically predicted, which was not considered to be significant. The results show that a few of the absorbers have significantly lower resonance frequencies from the intended design of the absorber. The reason for the difference was caused by the incorrect mass of the lower nut, which is used to attach to the absorber to the panel that was cut from bar stock and tapped with an M6 thread, and was not accurately machined to the precise height. The height of this nut varied slightly which alters the mass of the system, which alters the measured resonance frequency of the absorber.

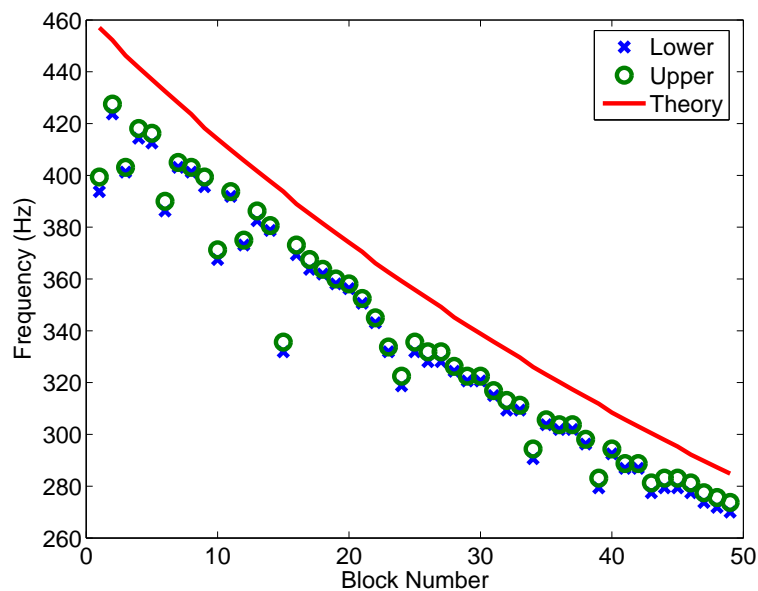


FIG. A.3: Predicted and measured resonance frequencies of the cantilevers.

It should be highlighted that no attempt was made to optimise the locations of the absorbers on the panel. The absorbers were attached to the panel in sequential order with the absorber that had the highest resonance frequency placed in the top left

corner of the panel, and the absorber with the lowest resonance frequency placed in the bottom right corner of the panel. Figure A.4 shows the location of the absorbers on the panel. Clearly this is not an optimal placement for the absorbers. The purpose of this experiment was not to optimise the location of the absorbers, but to test whether there would be any increase in the transmission loss of the panel when the absorbers were attached to the panel.

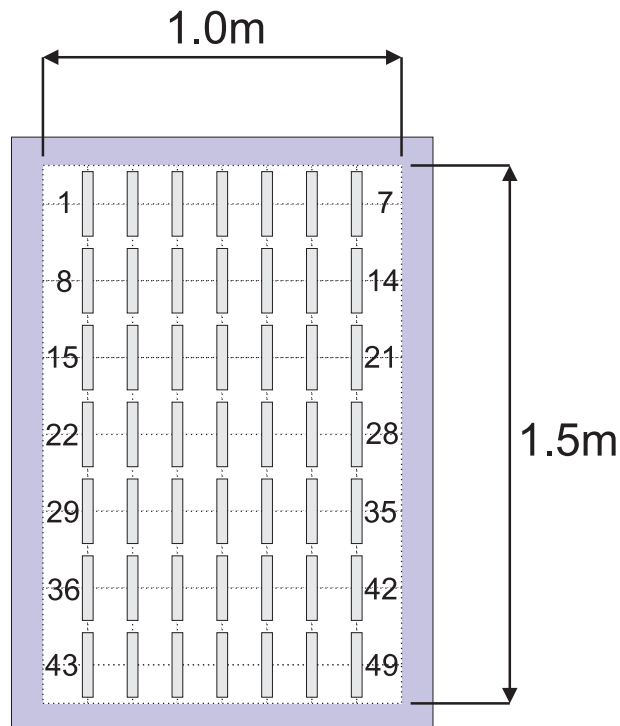


FIG. A.4: Location of the cantilevers attached to the clamped panel, with the numbers next to the beams indicating the cantilever absorber number.

The laser vibrometer was used to obtain vibration measurements of the panel. There are two main advantages of using the laser vibrometer compared to using accelerometers: 1) no additional mass is placed on the structure which would alter the vibration response of the structure, and 2) the scanning laser vibrometer enables numerous vibration measurements of the panel to be made relatively easily.

Figure A.5 shows a picture of the Polytec laser vibrometer software showing the grid of $17 \times 17 = 289$ measurement locations super-imposed on the panel with the cantilever absorbers.

Figure A.6 shows the measurement locations for the 49 cantilevers. Each cantilever

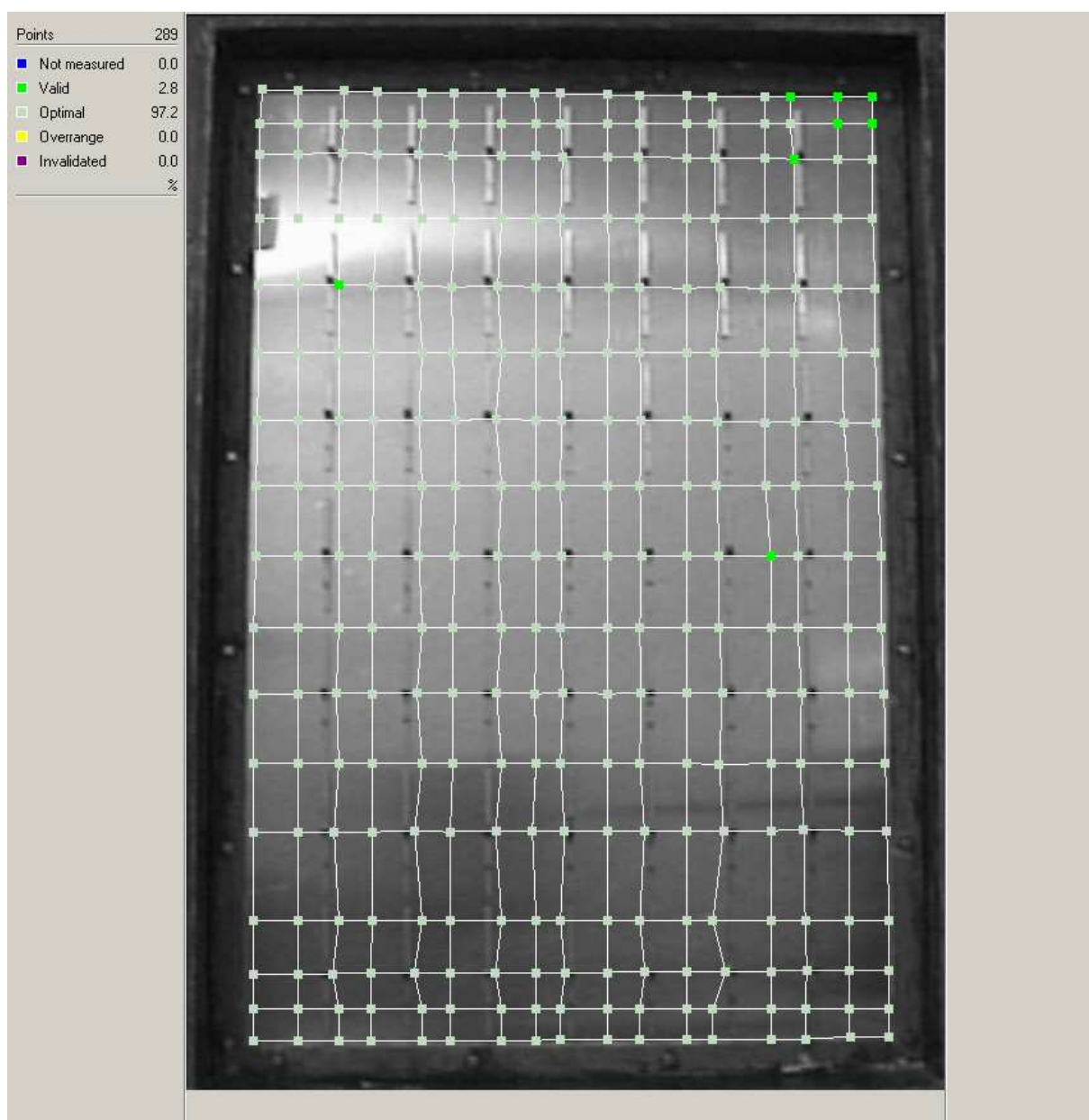


FIG. A.5: Screen capture of the Polytec software showing the grid of the 289 measurement locations on the panel.

had 5 measurement points: at the tip, mid-span, on the bolt, mid-span, at the tip.

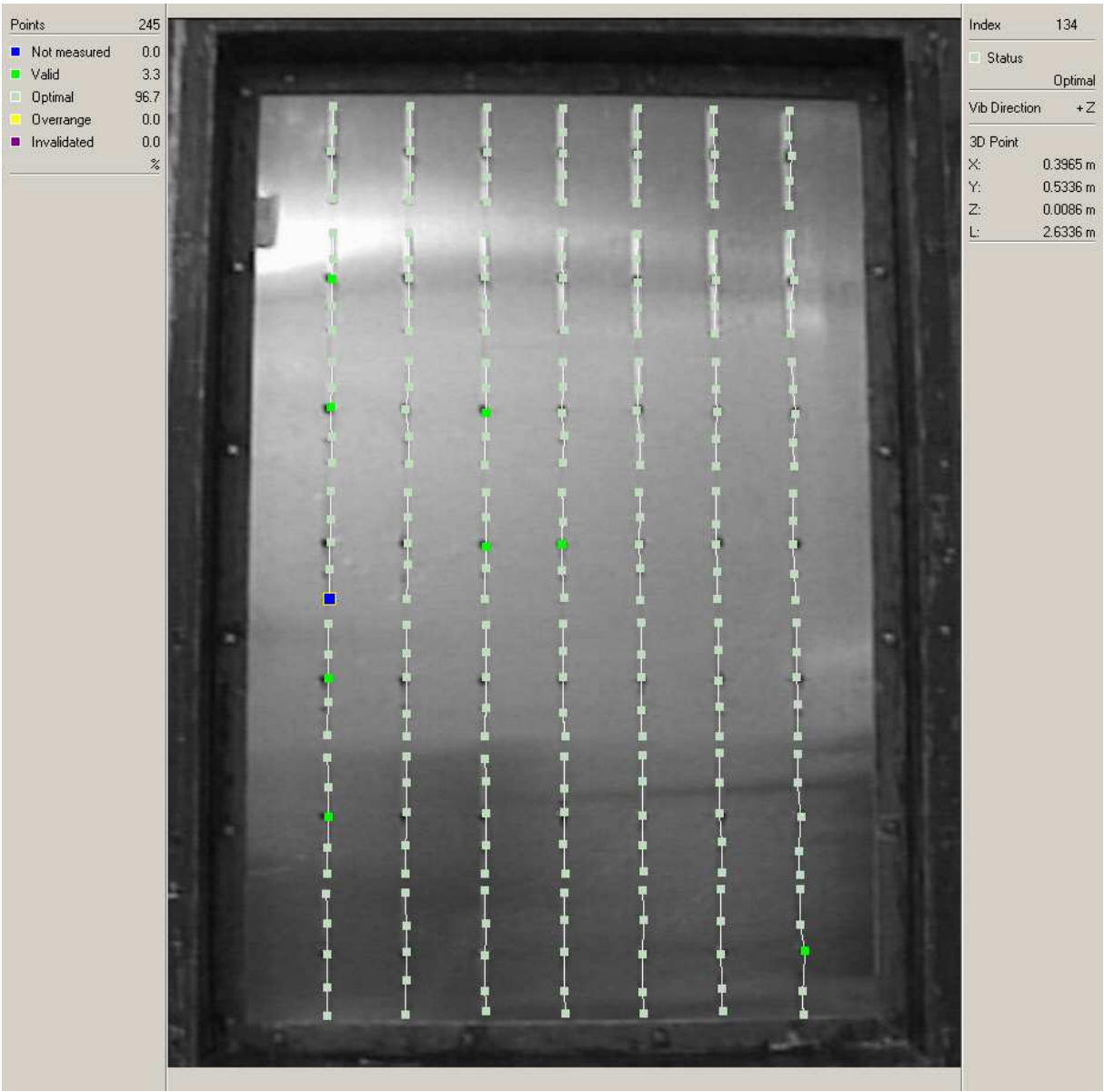


FIG. A.6: Screen capture of the Polytec software showing the 5 measurement locations on each of the 49 cantilevers.

A.3.3 Results

Figure A.7 shows the transmission loss for the system for the following configurations:

- experimentally measured transmission loss for the bare panel with no absorbers attached
- experimentally measured transmission loss for the panel with cantilever absorbers attached
- theoretically predicted transmission loss using Eq.(A.1) for an infinite panel
- theoretically predicted transmission loss using Eq.(A.2) for a finite panel

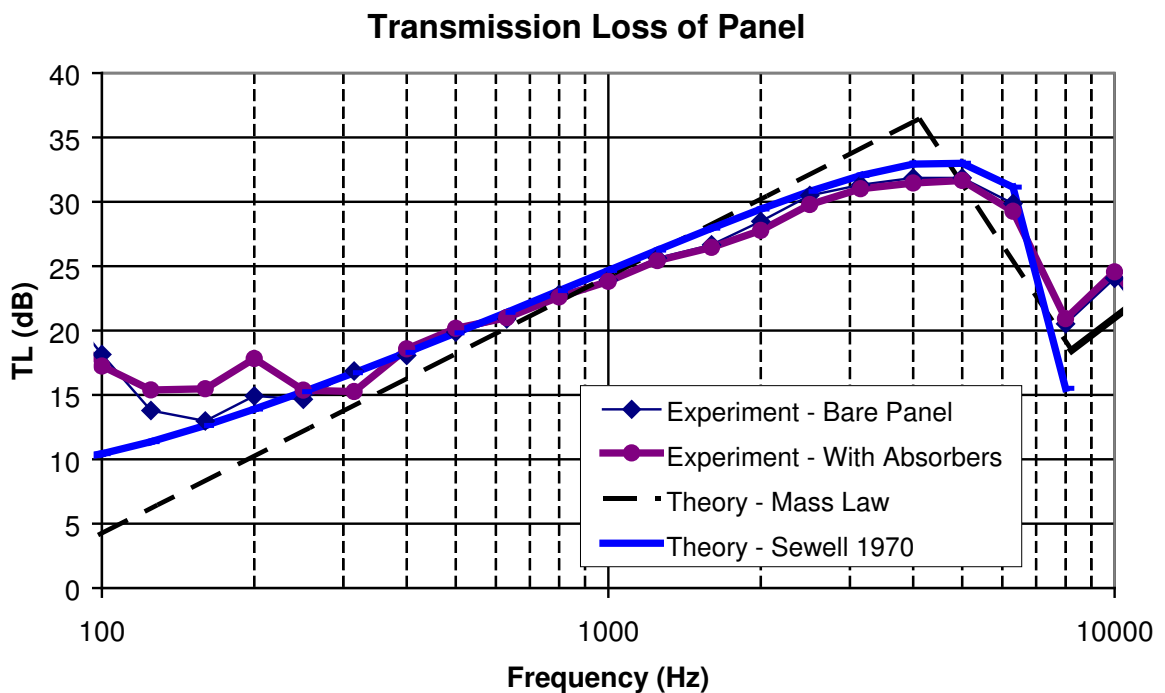


FIG. A.7: Transmission loss of the panel for the simple mass-law theory for an infinite panel, theory described by Sewell [36] and Fahy [12] for a finite panel, experimentally measured TL for a bare panel (no absorbers attached), and experimentally measured TL with the cantilevers absorbers attached.

The curve for the theoretical model of the transmission loss of an infinite panel has a slope of 6dB per octave, which does not reflect the experimentally measured transmission loss of the finite panel. The results show that the experimentally measured

transmission loss closely follows the predictions for the finite panel (shown in the figure as the blue thick line).

The area of the test aperture is approximately $1.0\text{m} \times 1.5\text{m}$, and the thickness of the panel is approximately 1.5mm. The mass of the panel in the aperture is $(1.0 \times 1.5 \times 0.0015 \times 2700 =) 6.075\text{kg}$. The total mass of cantilevers that were attached to the panel was 1.178kg, which is approximately 20% of the total mass of the panel. If the mass of the cantilevers were simply 'smeared' over the panel, the equivalent thickness of the panel would be 1.79mm. Hence from Eq. (A.2) the mass-law equation would predict an additional 1.5dB increase in transmission loss due to the increase in mass and panel thickness. However, the results show that there was a 2.5dB and 2.8dB increase in the TL in the 160Hz and 200Hz one-third octave band, respectively. Hence this result shows that there was significant improvement in the transmission loss when using the absorbers than the mass law would predict, even though no attempt was made to optimise the locations of the absorbers.

The non-contact laser vibrometer was used to measure the velocity of the panel at 289 locations, as shown in Figure A.5. Figure A.8 shows the operating deflection shape of the panel at 60Hz. The figure shows that the panel is vibrating in the 3,3 mode.

The average velocity is calculated by the summation of the squared velocity at each measurement point, divided by the number of measurement points, and then converted to decibels ($10 \times \log_{10}(\text{velocity})^2$). The results for the 'cantilever on frame' were obtained by removing absorber number 49 (which has the lowest resonance frequency) from the panel and mounting the absorber to the wall partition that divides the two reverberation chambers and measuring the velocity of the beams at 5 points along the length of the absorber.

Figure A.10 shows the same results as Figure A.9 only using a narrower range for the axes.

The results show that the absorbers (green dashed curve) had the greatest effect at reducing the average velocity of the panel in the 200Hz one-third octave band, com-

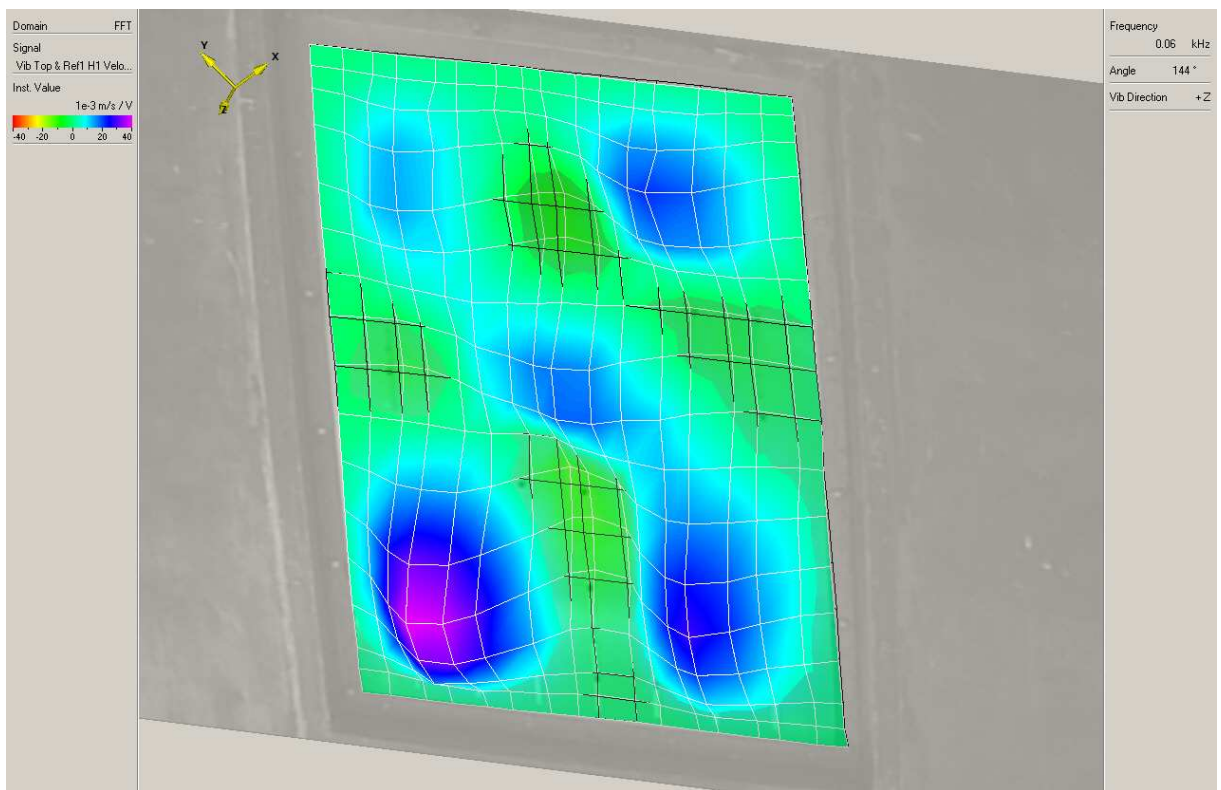


FIG. A.8: Displacement plot of the panel at 60Hz.

pared to the bare panel.

Figure A.11 presents the same results as Figure A.10 only using a narrow band frequency resolution. It is difficult to identify any trends from this figure, but was included in this report for completeness.

It can be seen in Figures A.9, A.10, A.10, and A.11 that there is a peak in the velocity response at approximately 450Hz. This is an unwanted artefact of the testing method and is unlikely to be related to the dynamics of the panel. Figure A.9 shows the vibration of the cantilever attached to the frame, which should be rigid, however it can be seen that there is a resonance in the 400Hz one-third octave band. Figure A.11 shows that the average velocity at 450Hz is identical for both sets of measurements. It is possible that the laser vibrometer has a resonance at this frequency and was excited by the high sound pressure levels (100dB) in the source room.

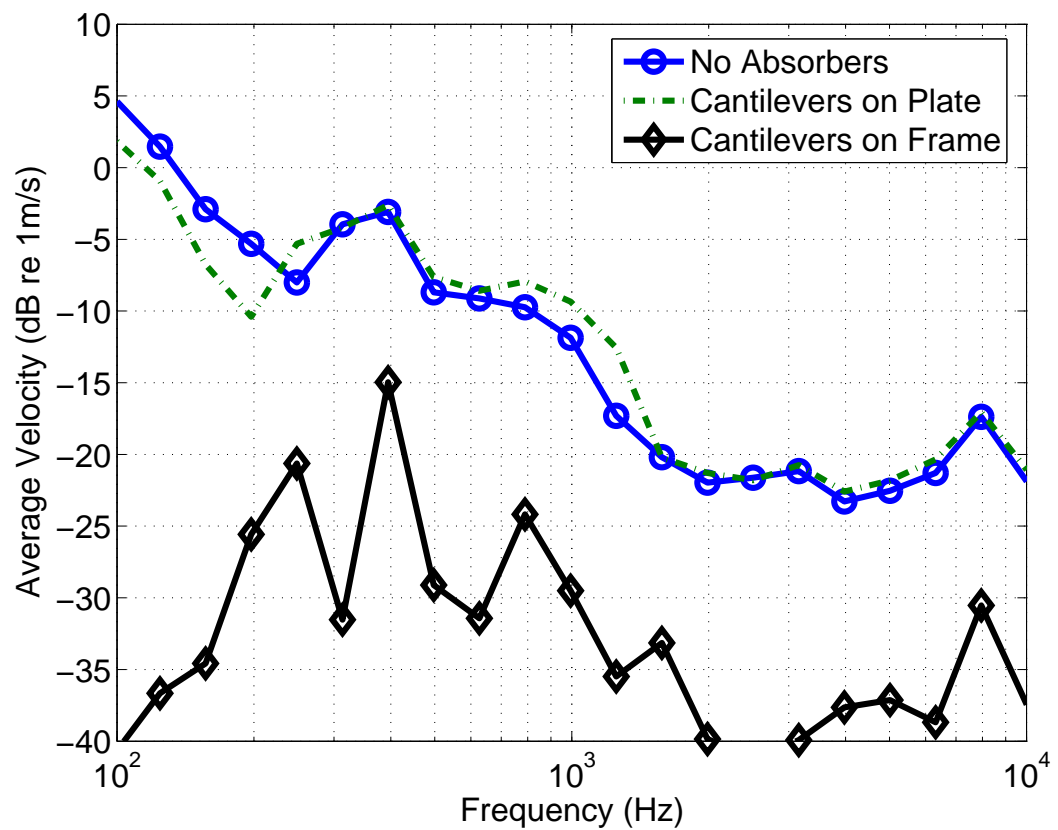


FIG. A.9: Average velocity in one-third octave bands of the panel for the bare panel (no absorbers attached), with the cantilevers attached, and the average velocity of an absorber that was rigidly mounted to the frame supporting the panel.

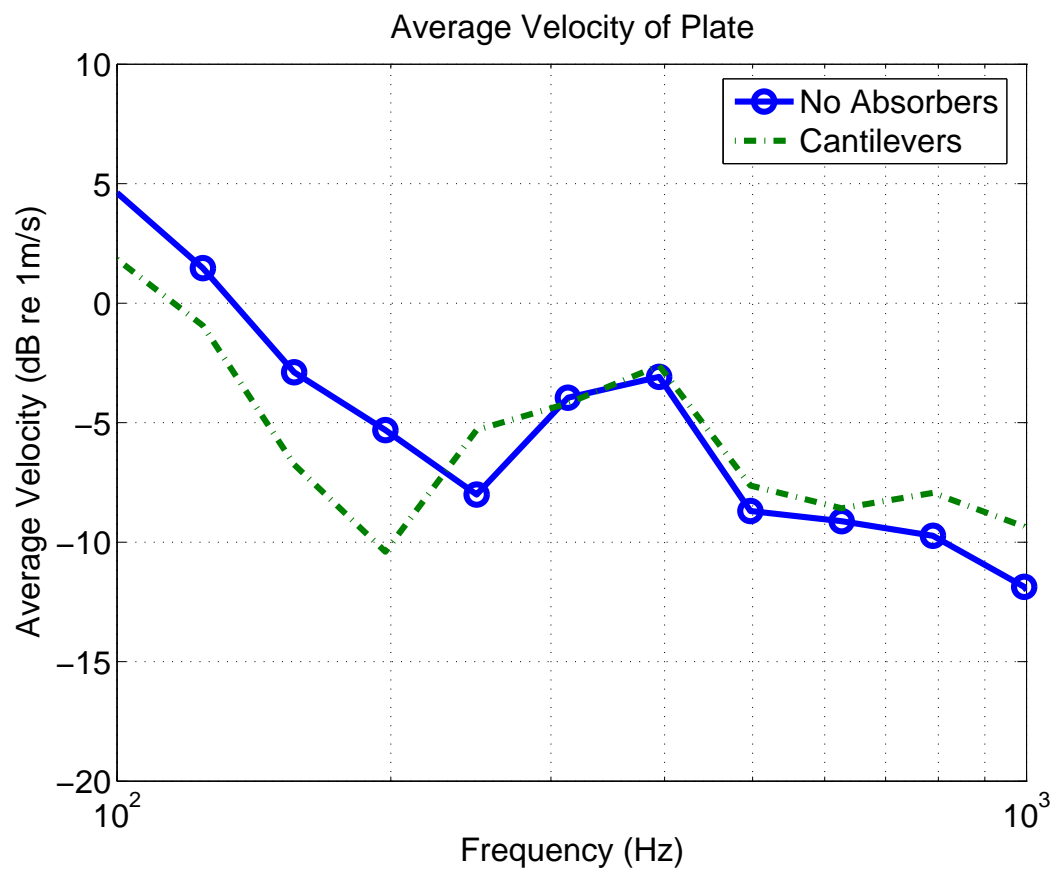


FIG. A.10: Average velocity in one-third octave bands of the panel.

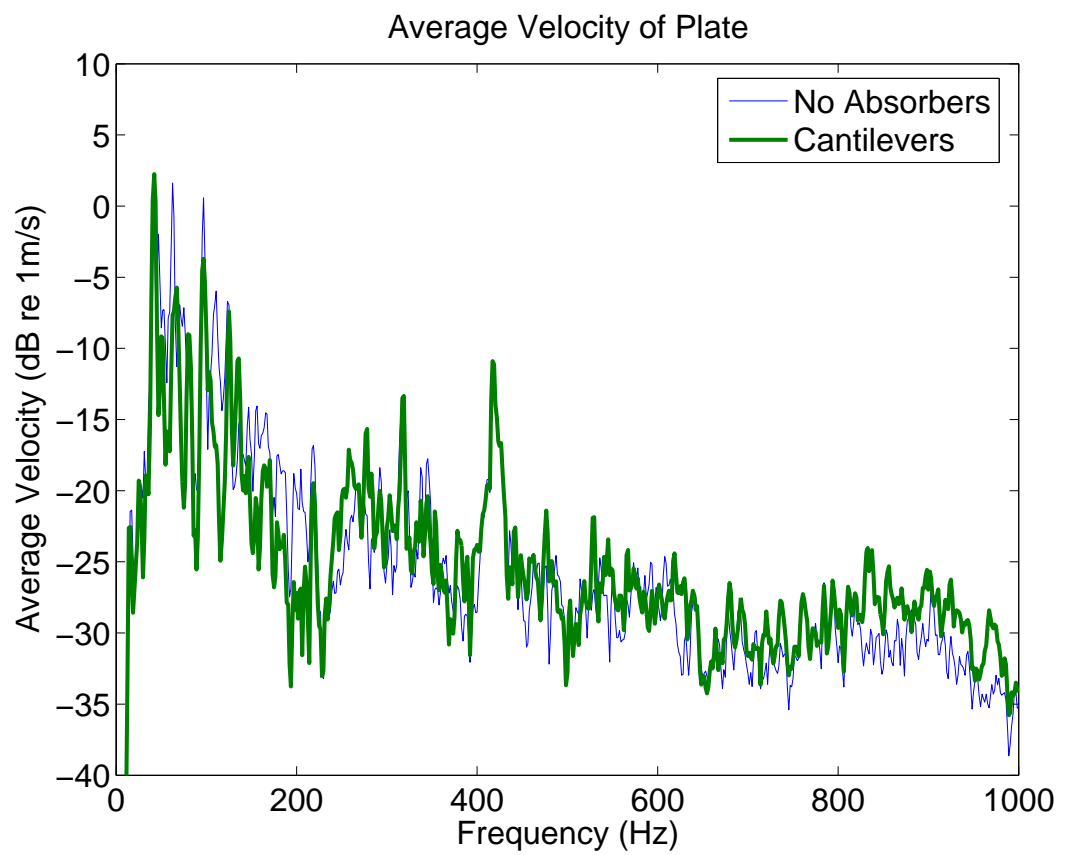


FIG. A.11: Experimentally measured average velocity of the panel shown using a narrow-band frequency resolution.

An additional measurement was conducted to measure the average velocity of the cantilever arms only, using a different set of measurement locations. This measurement was taken by using the scanning laser vibrometer and measuring the vibration of all 49 absorbers at 5 locations on each absorber. The measurement locations are shown in Figure A.6. The purpose of this measurement was to measure the vibration of the arms of the cantilevers and could be used to estimate the effect of the absorbers acting as un baffled vibrating beam acoustic sources, although this has not been attempted in this report.

Figure A.12 shows the operating deflection shape of the cantilevers at 220Hz. The use of the laser vibrometer enables the identification of the vibration modes of each cantilever. The figure shows that some of the cantilevers on the second from the top row of absorbers are vibrating in a torsional mode, where one arm of the cantilever is raised and the other arm is lowered.

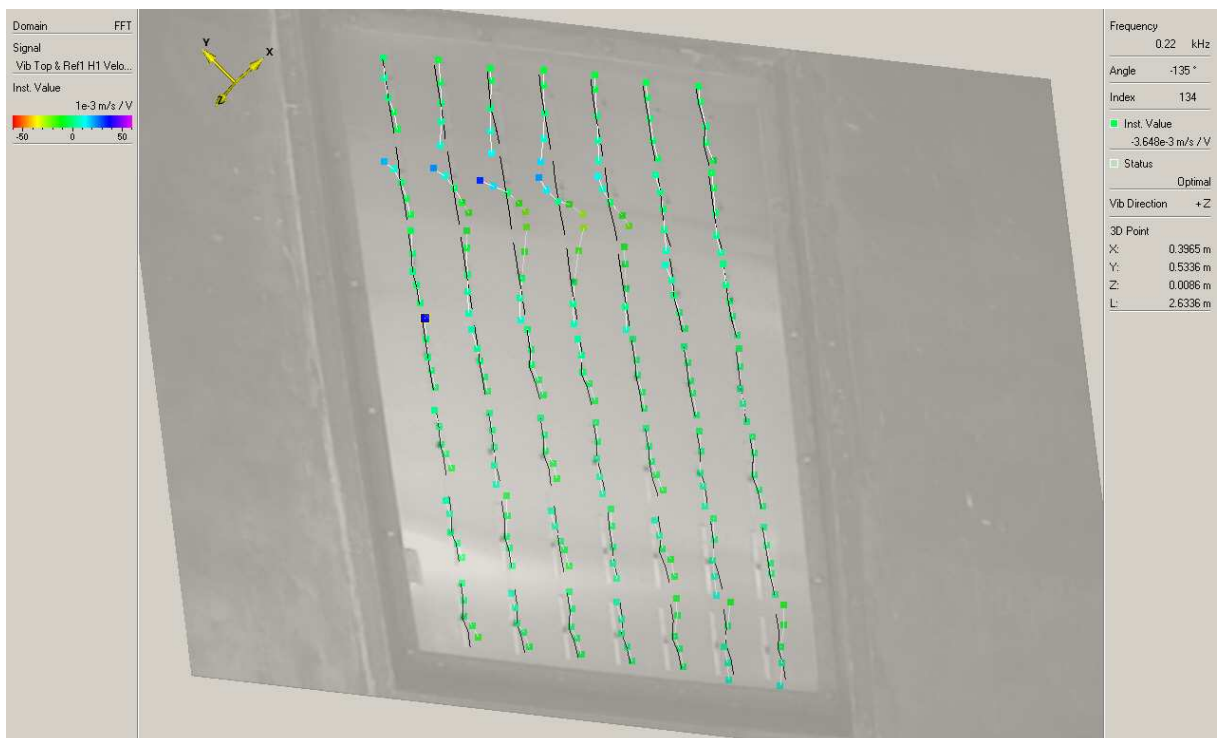


FIG. A.12: Displacement plot of the cantilevers at 220Hz.

Figure A.13 shows the same results as Figure A.9 with one additional curve for the average velocity of the cantilevers only.

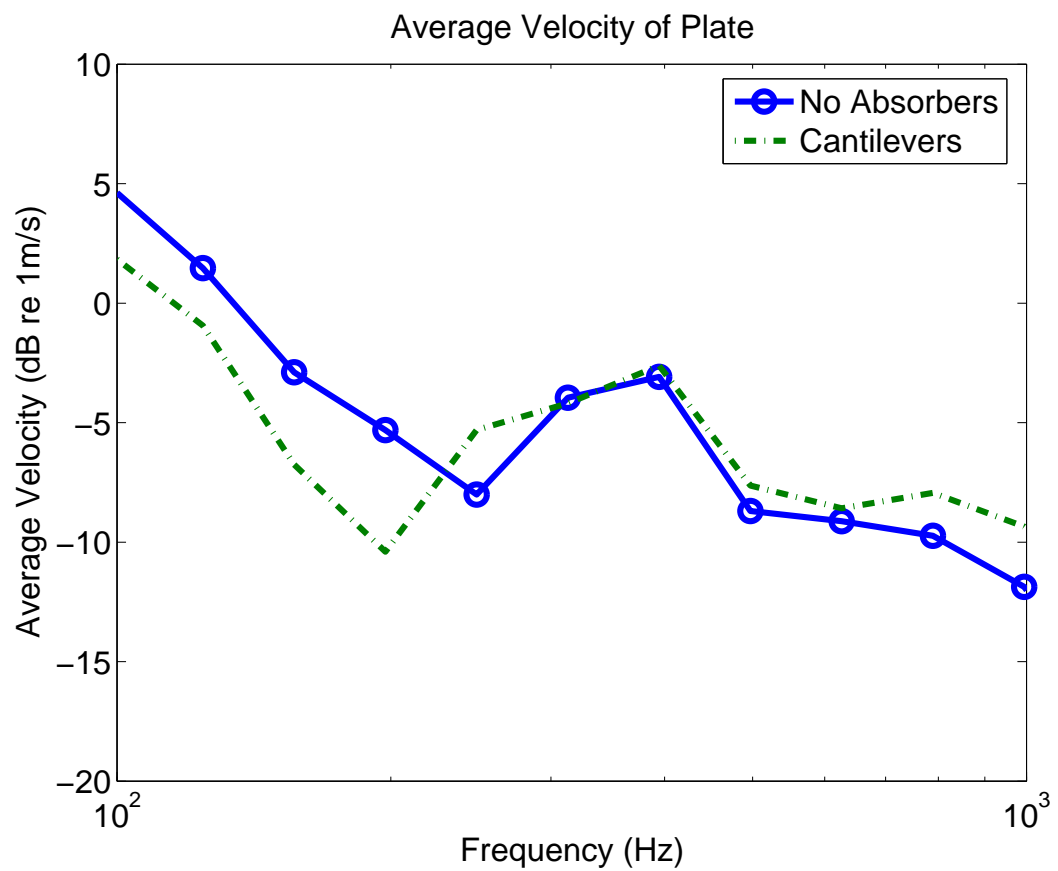


FIG. A.13: Average velocity of the panel in one-third octave bands.

A.4 Conclusions

The preliminary experimental results presented here show the benefit of using tuned vibration absorbers that have a continuous distribution of resonance frequencies. Although no attempt was made to optimise the location of the absorbers, the experimental results clearly showed the increase in transmission loss was greater than the increase in transmission loss due to mass-law effect alone.

Further work is required to

- complete the experimental testing for absorbers that have both translational and rotation degrees of freedom,
- determine the effect of using blocking masses that have the same weight as the cantilevers,
- compare the experimental results with a mathematical model to predict the transmission loss of the panel with and without the absorbers.

Appendix B

Properties of the Acoustic Chambers

Table B.1: Acoustic properties of the source room

Dimensions	6.085 x 5.175 x 3.355 m
Volume	105.6 m ³
Surface Area	138.5 m ²
Opening Area	9.71 m ²
Small Test Panel Opening	1100 wide x 1605 tall mm
Small Test Panel Size	1000 wide x 1505 tall mm (inside clamping frame)
Volume between chambers	9.42 m ³
Rotating Diffuser	Hemi-conical shape
	2.5m height
	1.5m diam top
	3.0m diam bottom
	Swept Volume 10.31m ³

Table B.2: Acoustic properties of the receiver room

Dimensions	6.840 x 5.565 x 4.720 m
Volume	179.7 m ³
Surface Area	193.2 m ² Including opening area
Opening Area	9.71 m ²
Small Test Panel Opening	1100 wide x 1605 tall mm
Small Test Panel Size	1000 wide x 1505 tall mm (inside clamping frame)
Volume between chambers	9.42 m ³
Rotating Diffuser	Hemi-cylindrical shape
	2.4m height
	3.5m diam
	Swept Volume 23.09 m ³

Figure B.1 shows the measured reverberation times in the receiver room of the transmission loss test facility, that were measured during the experimental testing of the panels described in Appendix A.

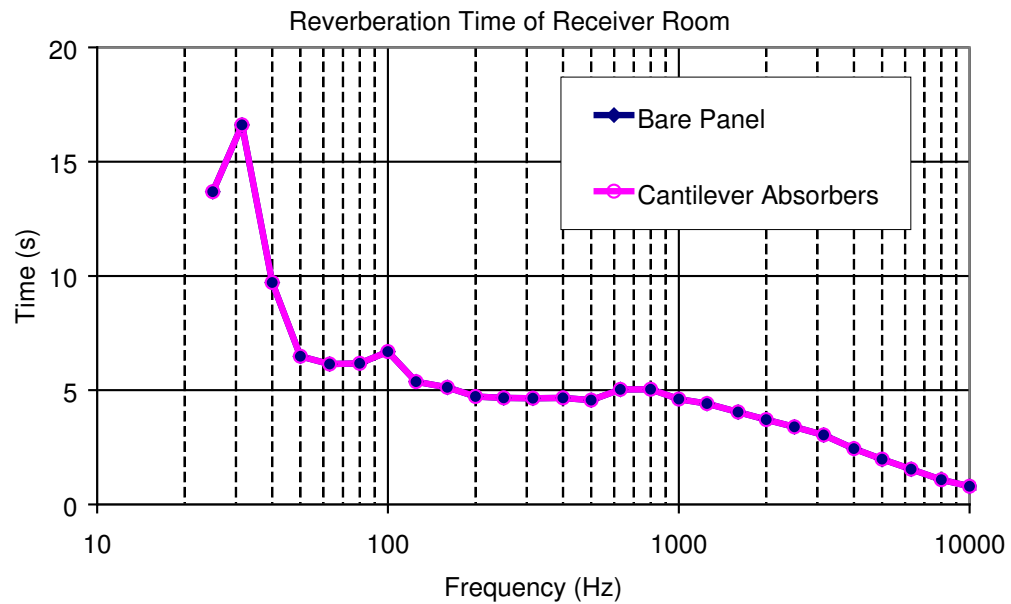


FIG. B.1: Experimentally measured reverberation times in the receiver room of the transmission loss testing facility.

Publications Arising from This Project

- [i] C.Q. Howard, R. Morgans, C.H. Hansen, and A.C. Zander. Optimisation of vibro-acoustic absorbers inside the payload bay of a launch vehicle using a parallel genetic algorithm and a distributed computing network. *Noise Control Engineering Journal*, 53(6):256–267, November-December 2005.
- [ii] C.Q. Howard, C.H. Hansen, and A.C. Zander. Vibro-acoustic noise control treatments for payload bays of launch vehicles: discrete to fuzzy solutions. *Applied Acoustics*, 66(11):1235–1261, November 2005.
- [iii] C.Q. Howard, C.H. Hansen, and A.C. Zander. Noise reduction of a rocket payload fairing using tuned vibration absorbers with translational and rotational dofs. In *Proceedings of Acoustics 2005*, pages 165–171, Busselton, Western Australia, Australia, 9-11 November 2005. Australian Acoustical Society, Australian Acoustical Society.
- [iv] C.Q. Howard, C.H. Hansen, and A.C. Zander. Optimisation of design and location of acoustic and vibration absorbers using a distributed computing network. In *Proceedings of Acoustics 2005*, pages 173–178, Busselton, Western Australia, Australia, 9-11 November 2005. Australian Acoustical Society, Australian Acoustical Society.
- [v] C.Q. Howard, C.H. Hansen, and A.C. Zander. Multi-variable optimisation of a vibro-acoustic system using a distributed computing network. In *ICSV12 - Proceedings of the 12th International Congress on Sound and Vibration*, Lisbon, Portugal,

11-14 July 2005. International Institute of Acoustics and Vibrations, International Institute of Acoustics and Vibrations. Paper No. 665.

- [vi] Rick Morgans, Ben Cazzolato, Anthony Zander, Colin Hansen, and Steven Griffin. Passive control of launch noise in rocket payload bays. In *ICSV9 - Proceedings of the 9th International Congress on Sound and Vibration*, Orlando, Florida, USA, 8-11 July 2002. International Institute of Acoustics and Vibrations, International Institute of Acoustics and Vibrations. Session Title: Rocket Noise and Vibration.

References

- [1] Colin H. Hansen, Anthony C. Zander, Ben S. Cazzolato, and Rick C. Morgans. Investigation of passive control devices for potential application to a launch vehicle structure to reduce the interior noise levels during launch: Final report for Stage 1. Technical report, Department of Mechanical Engineering, University of Adelaide, Adelaide, S.A. 5005, Australia, 14 November 2000. Contract Number: F6256200M9068.
- [2] Colin H. Hansen, Anthony C. Zander, Ben S. Cazzolato, and Rick C. Morgans. Investigation of passive control devices for potential application to a launch vehicle structure to reduce the interior noise levels during launch: Preliminary report for Stage 2. Technical report, Department of Mechanical Engineering, University of Adelaide, Adelaide, S.A. 5005, Australia, 14 February 2001. Contract Number: F6256299M9179.
- [3] Colin H. Hansen, Anthony C. Zander, Ben S. Cazzolato, and Rick C. Morgans. Investigation of passive control devices for potential application to a launch vehicle structure to reduce the interior noise levels during launch: Final report for Stage 2. Technical report, Department of Mechanical Engineering, University of Adelaide, Adelaide, S.A. 5005, Australia, 31 May 2001. Contract Number: F6256299M9179.
- [4] Carl Olsard, Rick Morgans, Anthony Zander, and Colin Hansen. Investigation of passive control devices for potential application to a launch vehicle structure to reduce the interior noise levels during launch: Final report for Stage 3A. Technical

- report, Department of Mechanical Engineering, University of Adelaide, Adelaide, S.A. 5005, Australia, September 2003. Contract Number : F6256299M9179.
- [5] Carl Q. Howard, Colin H. Hansen, Rick Morgans, and Anthony C. Zander. Investigation of passive control devices for potential application to a launch vehicle structure to reduce the interior noise levels during launch: Final report for Stage 3B. Technical report, Department of Mechanical Engineering, University of Adelaide, Adelaide, S.A. 5005, Australia, November 2003. Contract Number: F62562-03-C-0029.
- [6] Carl Q. Howard, Colin H. Hansen, and Anthony C. Zander. Investigation of passive control devices for potential application to a launch vehicle structure to reduce the interior noise levels during launch: Report for Stage 4, Tasks 1 and 2. Technical report, Department of Mechanical Engineering, University of Adelaide, Adelaide, S.A. 5005, Australia, July 2004. Contract Number: F62562-03-C-0029, Solicitation Number: F62562-03-R-0058.
- [7] Carl Q. Howard, Colin H. Hansen, and Anthony C. Zander. Investigation of passive control devices for potential application to a launch vehicle structure to reduce the interior noise levels during launch: Report for Stage 4, Tasks 3 and 4. Technical report, School of Mechanical Engineering, University of Adelaide, Adelaide, S.A. 5005, Australia, 14 September 2005. Contract Number: FA5209-05-P-0109, Purchase Request: F7AFOS42990200.
- [8] Carl Q. Howard, Colin H. Hansen, and Anthony C. Zander. Investigation of passive control devices for potential application to a launch vehicle structure to reduce the interior noise levels during launch: Report for Stage 4, Task 5. Technical report, School of Mechanical Engineering, University of Adelaide, Adelaide, S.A. 5005, Australia, 25 May 2006. Contract Number: FA5209-05-P-0109, Purchase Request: F7AFOS42990200, which is this report here.
- [9] S. Griffin, S. Lane, and D. Leo. Innovative vibro-acoustic control approaches in

- space launch vehicles. In *Inter-Noise 2000: The 29th International Congress and Exhibition on Noise Control Engineering*, number IN2000/737, Nice, France, 27-30 August 2000. INCE, INCE.
- [10] B. Henderson, C. Gerhart, S. Lane, and E. Jensen. Vibro-acoustic launch protection experiment (VALPE). *Journal of the Acoustical Society of America*, 114(4):2384, 2003.
- [11] Futron Corporation. Space transportation costs: Trends in price per pound to orbit 1990–2000. Technical report, Futron Corporation, 7315 Wisconsin Avenue, Suite 900W, Bethesda, Maryland 20814, 301-913-9372, <http://www.futron.com>, 6 September 2002.
- [12] Frank J. Fahy. *Sound and Structural Vibration: Radiation, Transmission and Response*. Academic Press, San Diego, California, USA, 1994. ISBN 0122476719.
- [13] The Condor Project Homepage.
<http://www.cs.wisc.edu/condor/>.
- [14] Rick Morgans, Ben Cazzolato, Anthony Zander, Colin Hansen, and Steven Griffin. Passive control of launch noise in rocket payload bays. In *ICSV9 - Proceedings of the 9th International Congress on Sound and Vibration*, Orlando, Florida, USA, 8-11 July 2002. International Institute of Acoustics and Vibrations, International Institute of Acoustics and Vibrations. Session Title: Rocket Noise and Vibration.
- [15] C.Q. Howard, R. Morgans, C.H. Hansen, and A.C. Zander. Optimisation of vibro-acoustic absorbers inside the payload bay of a launch vehicle using a parallel genetic algorithm and a distributed computing network. *Noise Control Engineering Journal*, 53(6):256–267, November-December 2005.
- [16] C.Q. Howard, C.H. Hansen, and A.C. Zander. Optimisation of design and location of acoustic and vibration absorbers using a distributed computing network. In *Proceedings of Acoustics 2005*, pages 173–178, Busselton, Western Australia, Aus-

- tralia, 9-11 November 2005. Australian Acoustical Society, Australian Acoustical Society.
- [17] C.Q. Howard, C.H. Hansen, and A.C. Zander. Multi-variable optimisation of a vibro-acoustic system using a distributed computing network. In *ICSV12 - Proceedings of the 12th International Congress on Sound and Vibration*, Lisbon, Portugal, 11-14 July 2005. International Institute of Acoustics and Vibrations, International Institute of Acoustics and Vibrations. Paper No. 665.
- [18] C.Q. Howard, C.H. Hansen, and A.C. Zander. Vibro-acoustic noise control treatments for payload bays of launch vehicles: discrete to fuzzy solutions. *Applied Acoustics*, 66(11):1235–1261, November 2005.
- [19] P. Gardonio, N.S. Ferguson, and F.J. Fahy. A modal expansion analysis of noise transmission through circular cylindrical shell structures with blocking masses. *Journal of Sound and Vibration*, 244(2):259–297, 5 July 2001.
- [20] C.Q. Howard, C.H. Hansen, and A.C. Zander. Noise reduction of a rocket payload fairing using tuned vibration absorbers with translational and rotational dofs. In *Proceedings of Acoustics 2005*, pages 165–171, Busselton, Western Australia, Australia, 9-11 November 2005. Australian Acoustical Society, Australian Acoustical Society.
- [21] P.A. Manning and S.A. Lane. A new predictive methodology for launch vehicle fill factors. In *Proceedings of the 9th International Congress of Sound and Vibration*, pages 583–590, Orlando, Florida, USA, 8-11 July 2002. International Institute of Acoustics and Vibrations.
- [22] Reiko Koganei, Qinzhong Shi, Shigemasa Ando, and Ichiro Hagiwara. The elucidation of mechanism of local sound pressure increase phenomenon. In Y. Park, J. Martin, and I. Mishiguchi, editors, *Computer Technology and Applications, 2004 ASME/JSME Pressure Vessels and Piping Conference*, volume 482, pages 201–206,

- San Diego, CA, United States, July 25-29 2004, 2004. ASME, Pressure Vessel and Piping Division, American Society of Mechanical Engineers.
- [23] Leo L. Beranek and Istvan L. Ver, editors. *Noise and vibration control engineering. Principles and applications*. John Wiley and Sons, U.S.A., 1992.
- [24] R. C. Potter. Correlation patterns of the acoustic pressure fluctuations on the s-ic vehicle due to the exhaust noise of the test and launch stand. Technical report, Wyle Labs, 1966. Report WR 66-15, Contract NAS8-20073-1.
- [25] Simon J. Estéve and Marty E. Johnson. Reduction of sound transmission into a circular cylindrical shell using distributed vibration absorbers and Helmholtz resonators. *Journal of the Acoustical Society of America*, 112(6):2840–2848, December 2002.
- [26] Simon J. Estéve. *Control of sound transmission into payload fairings using distributed vibration absorbers and Helmholtz resonators*. PhD thesis, Virginia Polytechnic Institute and State University, 6 May 2004.
- [27] S. Griffin, S.A. Lane, C.H. Hansen, and B.S. Cazzolato. Active structural-acoustic control of a rocket fairing using proof-mass actuators. *Journal of Spacecraft and Rockets*, 38(2):219–225, March/ April 2001.
- [28] H. Defosse and M.A. Hamdi. Vibro-acoustic study of Ariane V launcher during lift-off. In *Inter-Noise 2000: The 29th International Congress and Exhibition on Noise Control Engineering*, number IN2000/486, Nice, France, 27-30 August 2000. INCE, INCE.
- [29] W.O. Hughes, A.M. McNelis, and H. Himelblau. Investigation of acoustic fields for the Cassini spacecraft: Reverberant versus launch environments. Technical Memorandum NASA/TM-2000-209387; E-11814; AIAA Paper 99-1985; NAS 1.15:209387,, NASA Center for AeroSpace Information (CASI), September 2000. Prepared for the 5th Aerocoustics Conference and Exhibit cosponsored by the

- American Institute of Aeronautics and Astronautics and the Confederation of European Aerospace Societies Bellevue, Washington, May 10-12, 1999.
- [30] W.O. Hughes, M.E. McNelis, and J.E. Manning. NASA LeRCs acoustic fill effect test program and results. NASA Technical Memorandum 106688, National Aeronautics and Space Administration, October 1994.
- [31] Jerry Manning. Fairing noise reduction for directive acoustic fields. In *Spacecraft and Launch Vehicle Dynamic Environments Workshop*, El Segundo, California, USA, 26-28 June 2001. The Aerospace Corporation.
- [32] S.A. Lane, R.E. Richard, and S.J. Kennedy. Fairing noise control using tube shaped resonators. *Collection of Technical Papers - AIAA/ASME/ASCE/AHS/ASC Structures, Structural Dynamics and Materials Conference*, 5:3778 – 3781, 2003.
- [33] Deyu Li and Jeffrey S. Vipperman. Noise control for a chambercore cylindrical structure using long t-shaped acoustic resonators. *The Journal of the Acoustical Society of America*, 114(4):2323–2323, 2003. URL <http://link.aip.org/link/?JAS/114/2323/3>.
- [34] David A. Bies and Colin H. Hansen. *Engineering Noise Control, Theory and Practice*. E and F Spon, 2nd edition, 1997.
- [35] L.E. Kinsler, A.R. Frey, A.B. Coppens, and J.V. Saunders. *Fundamentals of Acoustics*. John Wiley and Sons, New York, USA, 4th edition, 2000. ISBN 0471847895.
- [36] E.C. Sewell. Transmission of reverberant sound through a single-leaf partition surrounded by an infinite rigid baffle. *Journal of Sound and Vibration*, 12(1):21–32, 1970.
- [37] Warren C Young. *Roark's Formulas for Stress and Strain*. McGraw Hill International, 6th edition, 1989.